Supporting Information

Supramolecular self-assembly of metal complex surfactants (MeCS) into micellar nanoscale reactors in aqueous solution

Ying Chen[a], Asia Matatyaho Ya'akobi[b], Thao Vy Nguyen[c], Shih-Chieh Kao[a], Julian G. West[a], Sibani Lisa Biswal[c], Yeshayahu Talmon[b], Angel A. Martí[a]*

[a]Department of Chemistry, Rice University, Houston, Texas, 77005, United States.

[b]Department of Chemical Engineering and The Russell Berrie Nanotechnology Institute, Technion-Israel Institute of Technology, 3200003 Haifa, Israel.

[c]Department of Chemical and Biomolecular Engineering, Rice University, Houston, TX 77005, United States.

Table of Contents

1. General considerations

All solvents and chemicals were obtained from Sigma Aldrich and Thermo Fisher Scientific unless otherwise stated, and they were used without any further purification. Absorbance spectra were recorded using a Shimadzu UV-2450 spectrophotometer. Fluorescence spectra were obtained with a HORIBA Nano log Spectrophotometer. Interfacial tension was studied using a CAM 200 KSV instrument. Quantum yields were determined using $[Ru(bpy)_3]Cl_2$ as a standard.[1] Time-resolved studies were performed using an Edinburgh Instruments OD470 single-photon counting spectrometer. 25 W PR160L 427 nm and 456 nm LEDs from Kessil Lights were used as the light source for the photoredox reactions. A Malvern Zen 3600 Zetasizer (633 nm laser) was used to measure the hydrodynamic diameter. ^{1}H NMR was recorded at 600 MHz, ^{19}F NMR was recorded at 565 MHz, and ^{13}C NMR was recorded at 151 MHz on a Bruker DRX-600 spectrometer. Cryo-TEM was performed using a Thermo Fisher Talos 200C HR-TEM equipped with a field emission gun. The vitrified specimens were maintained inside the microscope at a temperature of -180 °C using a Gatan 626 cryo-holder. Images were recorded digitally by an FEI Falcon III direct-imaging camera and the TIA software. A low-dose-imaging mode was applied to reduce electron-beam radiation damage. Image contrast was enhanced with the help of the "Volta phase-plate" of the TEM.[2]

2. Synthesis and characterization of Ru MeCSs

Scheme S1. Synthesis of ligands

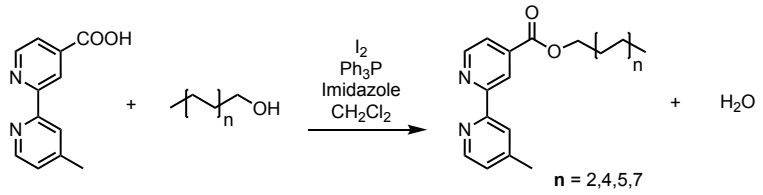

The ligands were synthesized based on the Garegg–Samuelsson reaction.[3] To a solution of I_2 (0.15 mmol) in dry DCM (4 mL), phosphine (0.15 mmol) was added, giving the solution a brown-yellow color. Then, imidazole (0.33 mmol) was added, changing the color to light yellow. Subsequently, carboxylic acid (0.1 mmol) was added, and the solution was stirred for 10 min at room temperature, and then the alcohol (0.15 mmol) was added. The mixture was stirred until complete consumption of the starting material was achieved (checked by thin-layer chromatography (TLC), around 12-24 h). Then, DCM was added, and the solution was washed with 2 N HCl and water before being dried with anhydrous Na_2SO_4, and the solvent was removed through rotavapor. The product was purified by column chromatography in a 1:1:1 mixture of DCM, hexanes, and acetone. The ligand's structures are confirmed by electrospray ionization mass spectrometry (ESI-MS).

Synthesis of surfactants

$[Ru(bpy)_2(bpy\text{-}R)]^{2+}$ was modified with long aliphatic chains following a previously reported protocol.[3] R represents

alkyl alcohols with four different chain lengths (6, 10, 12, and 16 carbon atoms). These alcohols were reacted with 4'-methyl-2,2'-bypyridine-4-carboxylic acid to form hydrophobic ligands (bpy-R) (Scheme S1). The ligand (bpy-R) then was refluxed with $Ru(bpy)_2Cl_2$. Hexanol, decanol, dodecanol, and hexadecanol were reacted with 4'-methyl-2,2'-bypyridine-4-carboxlic acid to form bpy-6C, bpy-10C, bpy-12C, and bpy-16C ligands, respectively. The synthesized ligands were then refluxed with $Ru(bpy)_2Cl_2$ to form ruthenium surfactants with an alkyl chain of different lengths ($[Ru(bpy)_2(bpy\text{-}R)]^{2+}$: R= 6C, 10C, 12C, and 16C). All compounds were purified by natural alumina column and characterized by ^1H nuclear magnetic resonance (NMR), ^{13}C NMR, and high-resolution mass spectrometry (HRMS). The proposed synthetic routes for $[Ru(bpy)_2(bpy\text{-}R)]^{2+}$ are presented below (**Scheme S2**).

Scheme S2. Synthesis of MeCSs

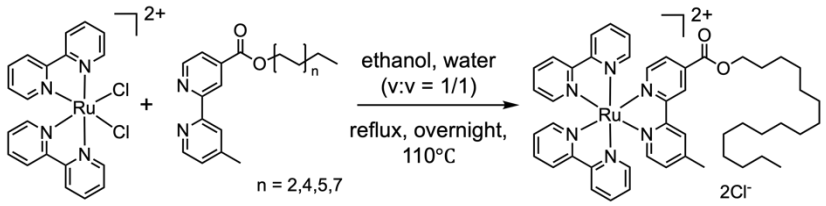

Cis-dichlorobis(2,2'-bipyridine)ruthenium(II) dihydrate:[4]

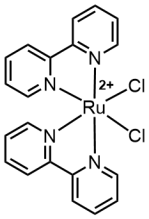

$Ru(bpy)_2Cl_2$ was synthesized based on a previously reported method.[4] $RuCl_3 \cdot 3H_2O$ (1.68 mmol), bipyridine (3.51 mmol), and LiCl (0.51 g) were refluxed in reagent grade DMF (9 mL) for 8 h with a magnetic stir bar. The reaction mixture was cooled to room temperature, and reagent-grade acetone (16 mL) was added. The reaction mixture was then cooled to 0 °C overnight. The mixture was then filtered, yielding a red-violet filtrate and a black crystalline product. The solid was washed three times with 10 mL portions of water, followed by three 10 mL portions of diethyl ether, and was subsequently dried by vacuum filtration. The spectral data were identical to those reported in the literature.[4]

^1H NMR (500 MHz, DMSO-d^6) δ 9.99 – 9.94 (m, 1H), 8.64 (d, J = 8.1 Hz, 1H), 8.49 (d, J = 8.1 Hz, 1H), 8.07 (td, J = 7.8, 1.6 Hz, 1H), 7.77 (ddd, J = 7.3, 5.7, 1.3 Hz, 1H), 7.72 – 7.65 (m, 1H), 7.51 (d, J = 5.7 Hz, 1H), 7.10 (ddd, J = 7.4, 5.8, 1.4 Hz, 1H).

Bis(bipyridine)ruthenium (hexyl 4'-methyl-[2,2'-bipyridine]-4-carboxylate) **Ru6C**:

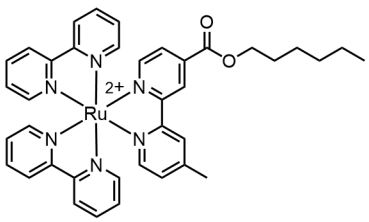

$Ru(bpy)_2Cl_2$ (27.33 mg, 0.10 mmol) and ligand **bpy-6C** (29.84 mg; 0.10 mmol) were suspended in EtOH/H_2O (1:1, 10 mL) with a magnetic stirrer. The mixture was purged with nitrogen for 20 minutes and refluxed for 8 h. After the reaction mixture was cooled to room temperature, the organic solvent was removed through rotary

evaporation. The resulting solid was purified by alumina chromatography using MeCN:H_2O= (10:0 - 10:1) as the eluent, yielding a black-red solid product that was dried in a vacuum oven at 40 °C. (38.0 mg, 48.5% yield)

^{1}H NMR (600 MHz, CN_3CN) δ 8.89 (d, *J* = 1.8 Hz, 1H), 8.65 (dd, *J* = 8.3, 3.1 Hz, 4H), 8.59 (d, *J* = 1.9 Hz, 1H), 8.07 (dddd, J = 9.4, 6.0, 3.0, 1.4 Hz, 4H), 7.91 (d, *J* = 5.8 Hz, 1H), 7.76 (dd, *J* = 5.9, 1.7 Hz, 1H), 7.72 (td, *J* = 5.0, 4.2, 1.5 Hz, 3H), 7.72 – 7.66 (m, 1H), 7.56 (d, *J* = 5.7 Hz, 1H), 7.43 – 7.35 (m, 3H), 7.29 (dd, *J* = 5.8, 1.8 Hz, 1H), 4.38 (t, *J* = 6.7 Hz, 2H), 2.56 (s, 3H), 1.78 (dt, *J* = 14.6, 6.8 Hz, 2H), 1.47 – 1.40 (m, 2H), 1.34 (ddt, *J* = 10.0, 6.3, 3.0 Hz, 4H), 0.92 – 0.86 (m, 3H). **^{13}C NMR** (151 MHz, CD_3CN) δ 164.21, 159.03, 157.61, 157.59, 157.51, 157.34, 156.35, 153.41, 152.32, 152.23, 152.20, 152.10, 151.41, 151.38, 139.06, 138.61, 138.57, 138.55, 129.43, 128.23, 128.21, 128.12, 128.03, 126.44, 126.34, 125.11, 125.07, 123.40, 117.91, 67.14, 31.70, 28.74, 25.82, 22.83, 20.75, 13.86. 238.1049. ESI^+-HRMS: calcd. for m/z $[C_{38}H_{38}N_6O_2Ru]^{2+}$: 356.1067; Found 356.1052.

Bis(bipyridine)ruthenium (decyl 4'-methyl- [2,2' bipyridine]-4-carboxylate) **Ru10C**:

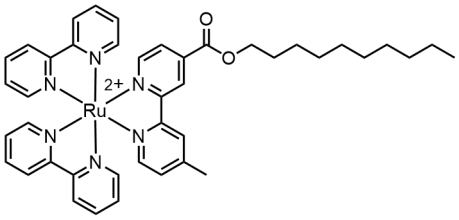

Compound **Ru10C** was synthesized according to the same procedure described for **Ru6C** but using ligand **bpy-10C**, yielding a black-red solid as the product, which was dried in a vacuum oven at 40 °C. (30.6 mg, 39.8% yield).

^{1}H NMR (600 MHz, CD_3CN) δ 8.88 (d, *J* = 1.8 Hz, 1H), 8.59 (d, *J* = 8.1 Hz, 4H), 8.57 (d, *J* = 1.8 Hz, 1H), 8.10 – 8.04 (m, 4H), 7.90 (d, *J* = 5.8 Hz, 1H), 7.76 (dd, *J* = 5.9, 1.8 Hz, 1H), 7.71 (td, *J* = 5.9, 1.4 Hz, 3H), 7.68 (dd, *J* = 5.7, 1.5 Hz, 1H), 7.56 (d, *J* = 5.8 Hz, 1H), 7.39 (dddd, *J* = 15.0, 7.3, 5.7, 1.4 Hz, 4H), 7.29 (dd, *J* = 5.8, 1.8 Hz, 1H), 4.38 (t, *J* = 6.7 Hz, 2H), 2.56 (s, 3H), 1.81 – 1.76 (m, 2H), 1.46 – 1.40 (m, 2H), 1.39 – 1.20 (m, 14H), 0.86 (t, *J* = 6.9 Hz, 3H). **^{13}C NMR** (151 MHz, CD_3CN) δ 164.57, 159.38, 157.97, 157.95, 157.88, 157.70, 156.70, 153.77, 152.65, 152.55, 152.52, 152.43, 151.77, 151.71, 151.45, 139.38, 138.98, 138.94, 138.92, 129.80, 128.59, 128.57, 128.48, 128.39, 126.81, 126.70, 125.56, 125.52, 125.29, 124.43, 123.75, 118.26, 67.48, 32.53, 30.15, 29.93, 29.83, 29.12, 26.49, 23.29, 21.11, 21.07, 14.31, 1.75, 1.58, 1.42, 1.25, 1.09, 0.92, 0.76. ESI^+-HRMS: calcd. for m/z $[C_{42}H_{46}N_6O_2Ru]^{2+}$: 384.1377; Found 384.1368.

Bis(bipyridine)ruthenium (dodecyl 4'-methyl-[2,2'-bipyridine]-4-carboxylate) **Ru12C**:

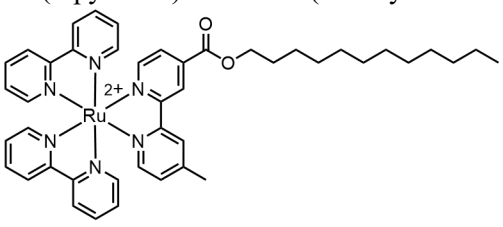

Compound **Ru12C** was synthesized according to the same procedure described for **Ru6C** but using ligand **bpy-12C**, yielding a black-red solid as the product, which was dried in a vacuum oven at 40 °C. (23.6 mg, 29.7% yield)

^{1}H NMR (600 MHz, CD_3CN) δ 8.90 (d, *J* = 1.7 Hz, 1H), 8.68 (dd, *J* = 8.2, 3.0 Hz, 4H), 8.60 (d, *J* = 1.9 Hz, 1H), 8.08 (tdd, *J* = 8.0, 4.4, 1.4 Hz, 4H), 7.91 (d, *J* = 5.8 Hz, 1H), 7.76 (dd, *J* = 5.9, 1.8 Hz, 1H), 7.72 (td, *J* = 5.8, 1.4 Hz, 3H),

7.69 (dd, *J* = 5.6, 1.4 Hz, 1H), 7.57 (d, *J* = 5.8 Hz, 1H), 7.43 - 7.37 (m, 4H), 7.29 (dd, *J* = 5.9, 1.8 Hz, 1H), 4.38 (t, *J* = 6.7 Hz, 2H), 2.56 (s, 3H), 1.81 - 1.75 (m, 2H), 1.38 - 1.20 (m, 18H), 0.86 (t, *J* = 7.0 Hz, 3H). **^{13}C NMR** (151 MHz, CD_3CN) δ 164.19, 159.02, 157.60, 157.50, 157.33, 156.35, 153.40, 152.33, 152.23, 152.19, 152.11, 151.41, 139.07, 138.60, 138.57, 138.54, 129.43, 128.21, 128.12, 126.45, 126.33, 125.07, 125.04, 124.80, 123.39, 117.91, 67.15, 32.20, 29.92, 29.91, 29.84, 29.79, 29.63, 29.48, 28.76, 26.14, 22.96, 20.75, 13.96. ESI$^+$-HRMS: calcd. for m/z $[C_{44}H_{50}N_6O_2Ru]^{2+}$: 398.1537; Found 398.1526.

Bis(bipyridine)ruthenium (hexadecyl 4'-methyl-[2,2'-bipyridine]-4-carboxylate) **Ru16C**:

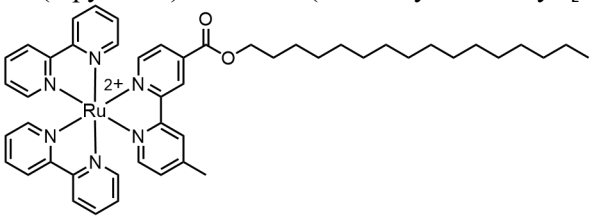

Compound **Ru16C** was synthesized according to the same procedure described for **Ru6C** but using ligand **bpy-16C**, yielding a black-red solid as the product, which was dried in a vacuum oven at 40 °C. (18.1 mg, 19.6% yield).

^{1}H NMR (600 MHz, CD_3CN) δ 8.94 (d, *J* = 1.7 Hz, 1H), 8.57 (s, 1H), 8.13 (d, *J* = 5.6 Hz, 1H), 8.07 (d, *J* = 1.3 Hz, 1H), 8.06 (s, 1H), 7.90 (dd, *J* = 5.6, 1.7 Hz, 1H), 7.84 (td, *J* = 7.8, 1.5 Hz, 2H), 7.81 (dt, *J* = 7.5, 2.4 Hz, 3H), 7.58 (d, *J* = 5.7 Hz, 2H), 7.37 (dd, *J* = 5.7, 1.7 Hz, 1H), 7.08 – 6.98 (m, 4H), 6.92 (tdd, *J* = 7.4, 4.5, 1.3 Hz, 2H), 6.27 (ddd, *J* = 18.5, 7.6, 1.2 Hz, 2H), 4.39 (t, *J* = 6.6 Hz, 2H), 2.56 (s, 3H), 1.78 (m, *J* = 6.8 Hz, 2H), 1.46 - 1.40 (m, 2H), 1.38 - 1.32 (m, 2H), 1.31 - 1.21 (m, 22H), 0.87 (t, *J* = 7.0 Hz, 3H). **^{13}C NMR** (151 MHz, CD_3CN) δ 168.37, 168.26, 164.44, 158.18, 155.63, 153.23, 152.63, 151.03, 150.98, 150.14, 145.06, 144.86, 141.08, 139.56, 132.53, 132.37, 131.34, 130.42, 128.21, 126.95, 125.84, 124.47, 124.42, 123.60, 123.57, 120.87, 118.26, 67.59, 32.58, 30.32, 30.28, 30.24, 30.15, 30.11, 30.01, 29.80, 29.09, 26.48, 23.33, 21.31, 14.33. ESI$^+$-HRMS: calcd. for m/z $[C_{48}H_{58}N_6O_2Ru]^{2+}$: 426.1849; Found 426.1840.

3. Critical micelle concentration (CMC) determination

The pendant drop method was used to determine the critical micelle concentration (CMC) of each surfactant. The surface tension between the water droplet and the air changes with concentration until the concentration reaches the CMC, then the surface tension becomes constant. A series of surfactant solutions at different concentrations were prepared. Interfacial tension was measured by using a CAM 200 KSV instrument. By measuring the surface tension of the sample droplet at each time spot and measuring the surface tension of the sample droplet at different concentrations, we have determined the CMC of each surfactant. The ruthenium surfactant solutions were prepared by direct dissolution in water.

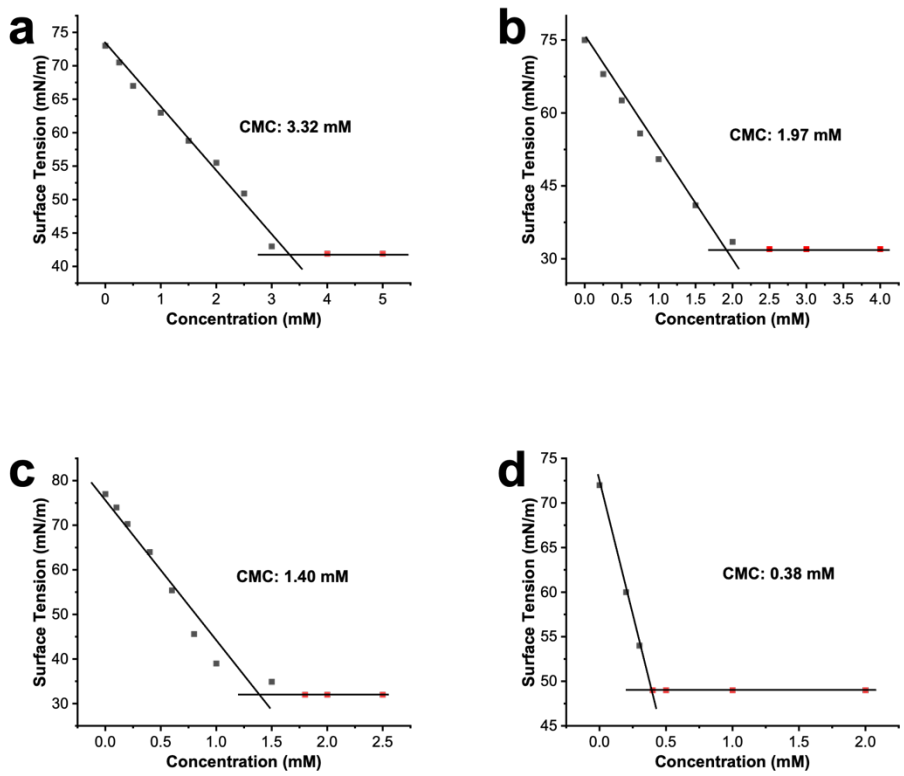

Figure S1. Surface tension measurements for Ru6C(a), Ru10C(b), Ru12C(c), and Ru16C(d).

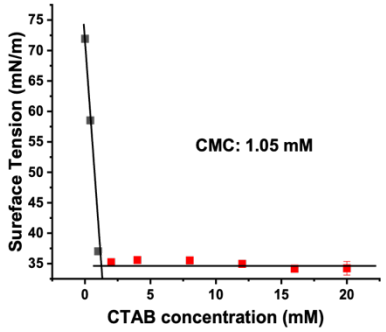

Figure S2. Surface tension measurements for mixed solutions of Ru16C and CTAB. Each CTAB solution contains 5 mol% Ru16C.

4. Methodology of Cryo-TEM experiments:

Cryo-TEM specimens were prepared in a controlled environment vitrification system (CEVS).[5] The CEVS was saturated with water vapor to prevent specimen drying and was maintained at 25 °C. A drop of ~3 µL was applied onto a perforated carbon film supported on a 3 mm copper TEM grid. The grids were treated with glow-discharge air plasma (Ted Pella, Inc.) to improve the wettability of the support. The drop was blotted with a filter paper to form a thin film

(<300 nm) and then vitrified by plunging into freezing ethane. Prior to the plunging, we let the specimen relax on the grid for 15-30 seconds to avoid flow-induced artifacts caused during the blotting.

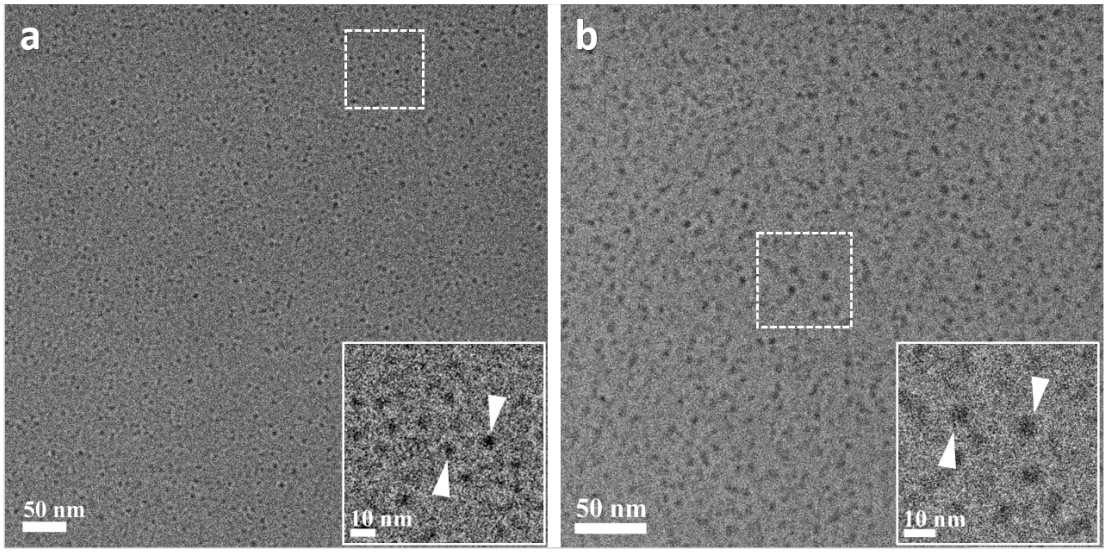

Figure S3. Cryo-TEM micrographs of Ru12C and Ru12C-CTAB in water. (a) 4 mM Ru12C micellar solution, and (b) a solution of 1 mM Ru12C and 20 mM CTAB. Dashed squares mark the magnified areas shown in the insets. Arrowheads point to globular surfactant micelles.

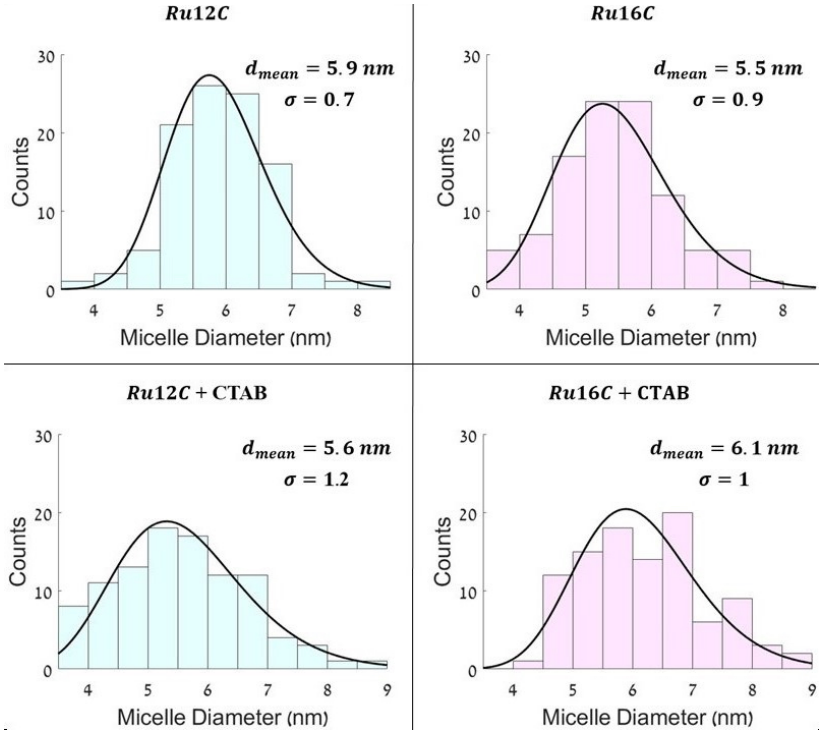

Figure S4. Statistical analysis results of the micelle diameter of Ru12C and Ru16C in water based on the Cryo-TEM images. For each micellar solution, the diameter of 100 micelles was measured.

5. DLS measurements

DLS samples were analyzed at 2 mM surfactant in water at 20°C, as shown in Figure S5. Additionally, all the samples were filtered with a 0.2 μm PTFE syringe filter before each measurement.

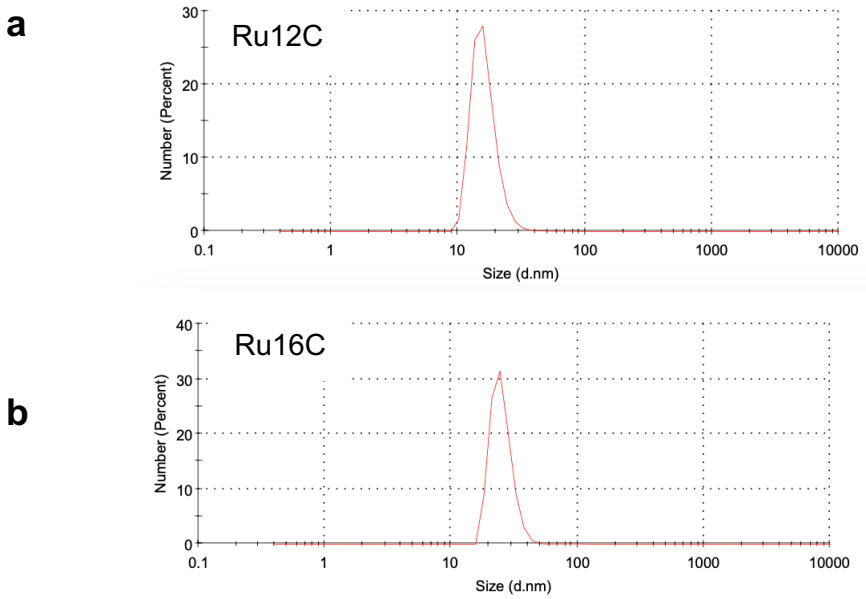

Figure S5. Hydrodynamic diameter of the Ru12C (**a**) and Ru16C micelles (**b**) measured by dynamic light scattering (DLS).

6. Absorption and emission spectra of ruthenium surfactants

Although all the measurements were performed below the CMC, surfactants can possibly still form aggregates that lead to quenching of the metal complex triplet state.[6,7] Additionally, the triplet state of these metal complexes can be quenched by molecular oxygen and, therefore, can influence the quantum yield and lifetime.[8] The formation of micelles and oxygen diffusion in the solution can also impact the steady-state photoluminescence of MeCSs as reported previously in the literature.[9,10] Thus, we also decided to determine the photophysical properties of each surfactant below and above CMC in deoxygenated water. Unfortunately, the inner-filter effect becomes an issue as the concentration of MeCS in the solution is increased. Additionally, self-quenching is possible due to the proximity of metal complexes in the micelle. To study the effect of micelle formation on the MeCSs without the high concentrations of MeCS needed to reach the CMC, we will use cetrimonium bromide (CTAB) as the diluent, which is a cationic surfactant with a 16-carbon alkyl chain. CTAB is optically transparent in the visible range and will form micelles together with the MeCSs. The incorporation of CTAB into our surfactants allowed us to study the photoluminescence properties of MeCSs within micelles.

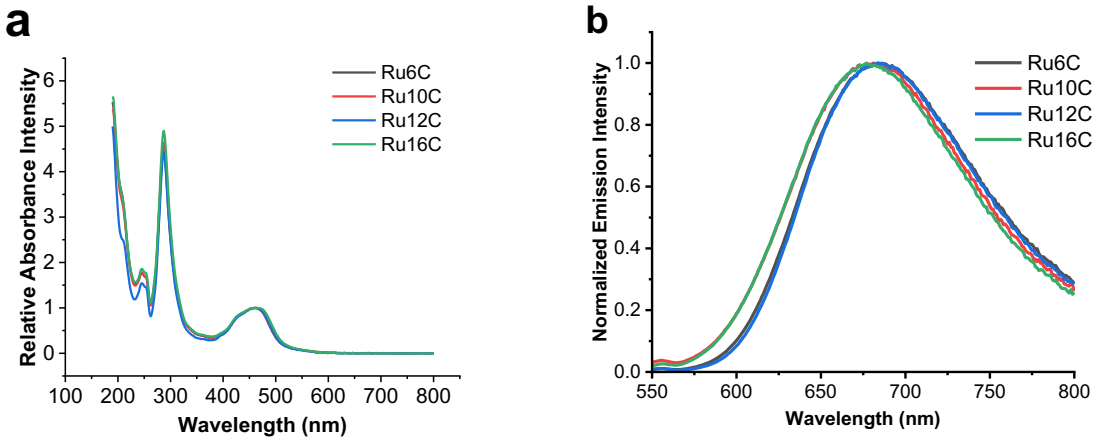

Figure S6. Normalized absorbance and emission spectra of Ru MeCSs (a, b) in water at 298K (λ_{exc} = 460 nm).

7. Photoluminescence quantum yield determination

The photoluminescence quantum yield (ϕ_{em}) of MeCSs was determined by using $[Ru(bpy)_3]Cl_2$ as a standard (ϕ_{em} = 0.04 in water) below CMC to avoid self-quenching.[11] The absorbance was kept below 0.05, avoiding the inner filter effect.[12] The photoluminescence quantum yield of MeCSs was then determined by Equation 1:[13]

$$\phi_{unk} = \phi_{std} \cdot \frac{A_{std}}{I_{std}} \cdot \frac{I_{unk}}{A_{unk}} \cdot \frac{n_{unk}^2}{n_{std}^2} \qquad (1)$$

where ϕ, A, I, and n represent the photoluminescence quantum yield, absorbance, integrated emission intensity, and refractive index of the solvent.[11,13,14]

8. Default reaction condition of hydroxytrifluoromethylation of styrene and setup

Hydroxytrifluoromethylation of styrene:

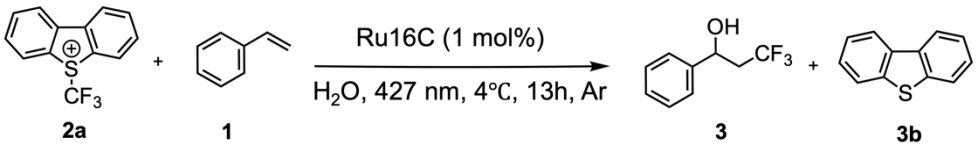

The photocatalytic reaction was carried in a reaction tube equipped with a magnetic stir bar. Ru16C (0.85 mg, 0.01 mmol), 5-(trifluoromethyl) dibenzothiophenium chloride (Umemoto's reagent, **2c**) (28.9 mg, 0.1 mmol), styrene (**1**) (11.5 mg, 0.11 mmol) and water (2 ml) were added into the reaction tube. The obtained solution was purged with Argon for three minutes and dipped into a water bath to maintain a stable temperature. The Umemoto's reagent was converted to the chloride salt using Amberlite IRA-410 ion exchange resin. An extra fan was equipped on the top of the reaction tube, and a 427 nm LED was placed about 3 cm away from it. The yellow solution was stirred at a 4°C fridge under a 427 nm LED irradiation. After 13 hours, the reaction mixture was extracted with methyl *tert*-butyl ether twice. The combined organic solution was dried by adding Na_2SO_4 and filtrated. The filtrate was concentrated under vacuum, and fluorobenzene (0.3 mmol) was added as the NMR internal standard; $CDCl_3$ was added as the solvent for the ^{19}FNMR yield determination. The isolated product was obtained by silica gel chromatography using hexane: EtOAc= (10:0 to 10:1) as the eluent, yielding a colorless oil product that was dried in a vacuum oven at 40 °C. (15.2 mg, 80% yield)

3,3,3-trifluoro-1-phenylpropan-1-ol **(3)**:[15]

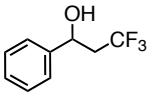

The spectral data were identical with those reported in the literature.[15]

^{1}H NMR (600 MHz, $CDCl_3$) δ 7.38 - 7.20 (m, 5H), 5.01 (dd, *J* = 9.1, 3.5 Hz, 1H), 2.66 - 2.48 (m, 1H), 2.48 - 2.29 (m, 1H). **^{19}F NMR** (565 MHz, $CDCl_3$) δ -63.76 (t, *J* = 10.6 Hz). **^{13}C NMR** (151 MHz, $CDCl_3$) δ 142.33, 128.91, 128.44, 126.82 (q, *J* = 277 Hz), 125.67, 68.89, 42.89 (q, *J* = 27.2 Hz).

3,3,3-trifluoro-1-(p-tolyl) propan-1-ol **(4)**:[16]

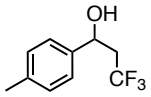

According to the default condition, compound **4** was synthesized according to the same procedure described for compound **3**, yielding a colorless oil (14.5 mg, 72% yield) as the product after purification with silica gel column chromatography (hexane/EtOAc = 50:1 to 5:1) The spectral data were identical with those reported in the literature.[16]

^{1}H NMR (600 MHz, $CDCl_3$) δ 7.26 (s, 2H), 7.20 (s, 2H), 5.05 (m, 1H), 2.63 (m, 1H), 2.44 (m, 1H), 2.36 (s, 3H). **^{19}F NMR** (565 MHz, $CDCl_3$) δ -63.75 (t, *J* = 11.0 Hz). **^{13}C NMR** (151 MHz, $CDCl_3$) δ 139.42, 138.26, 129.51, 127.82 (q, *J* = 277 Hz), 125.61, 68.66, 42.73 (q, *J* = 27.0 Hz), 29.71, 21.13.

1-(4-(tert-butyl) phenyl)-3,3,3-trifluoropropan-1-ol **(5)**:[15]

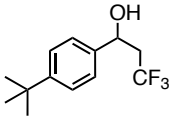

According to the default condition, compound **5** was synthesized according to the same procedure described for compound **3**, yielding a colorless oil (16.1 mg, 65% yield) as the product after purification with silica gel column chromatography (hexane/EtOAc = 50:1 to 5:1) The spectral data were identical with those reported in the literature.[15]

^{1}H NMR (600 MHz, $CDCl_3$) δ 7.41 (d, *J* = 8.5 Hz, 2H), 7.31 (d, *J* = 8.2 Hz, 2H), 5.06 (d, *J* = 12.3 Hz, 1H), 2.73 - 2.58 (m, 1H), 2.53 - 2.40 (m, 1H), 1.32 (s, 9H). **^{19}F NMR** (565 MHz, $CDCl_3$) δ -63.78 (t, *J* = 10.6 Hz). **^{13}C NMR** (151 MHz, $CDCl_3$) δ 151.55, 139.37, 125.97 (q, *J* = 277 Hz), 125.78, 125.42, 68.66, 68.64, 68.61, 68.58, 42.77 (q, *J* = 26.8 Hz), 34.61, 31.31.

3,3, 3-trifluoro-1-(4-methoxyphenyl) propan-1-ol **(6)**:[15]

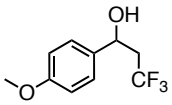

According to the default condition, compound **6** was synthesized according to the same procedure described for compound **3**, yielding a colorless oil (17.4 mg, 79% yield) as the product after purification with silica gel column chromatography (hexane/EtOAc = 50:1 to 5:1) The spectral data were identical with those reported in the literature.[15]

^{1}H NMR (600 MHz, $CDCl_3$) δ 7.34 - 7.27 (m, 2H), 6.90 (d, *J* = 9.6 Hz, 2H), 5.03 (dd, *J* = 8.9, 3.8 Hz, 1H), 3.81 (s, 3H), 2.62 (s, 1H), 2.50 - 2.36 (m, 1H). **^{19}F NMR** (565 MHz, $CDCl_3$) δ -63.60 (t, *J* = 11.0 Hz). **^{13}C NMR** (151 MHz, $CDCl_3$) δ 159.65, 134.51, 130.67, 127.00, 126.00 (q, *J* = 276 Hz), 68.46, 55.25, 42.80 (q, *J* = 26.8 Hz).

3,3,3-trifluoro-1-(4-fluorophenyl) propan-1-ol **(7)**:[15]

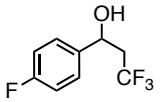

According to the default condition, compound **7** was synthesized according to the same procedure described for compound **3**, yielding a colorless oil (17.1 mg, 82% yield) as the product after purification with silica gel column chromatography (hexane/EtOAc = 50:1 to 5:1) The spectral data were identical with those reported in the literature.[15]

^{1}H NMR (600 MHz, $CDCl_3$) δ 7.41 – 7.26 (m, 2H), 7.07 (m, 2H), 5.08 (dd, *J* = 8.9, 3.7 Hz, 1H), 2.62 (m, 1H), 2.43 (m, 1H). **^{19}F NMR** (565 MHz, $CDCl_3$) δ -63.73 (t, *J* = 10.6 Hz), -113.65. **^{13}C NMR** (151 MHz, $CDCl_3$) δ 163.59, 161.61, 127.44, (d, *J* = 8.2 Hz), 121.57, 115.9 (d, *J* = 21.5 Hz), 68.22, 42.90 (q, *J* = 27.2 Hz).

1-(4-chlorophenyl)-3,3,3-trifluoropropan-1-ol **(8)**:[15]

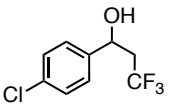

According to the default condition, compound **8** was synthesized according to the same procedure described for compound **3**, yielding a colorless oil (17.0 mg, 76% yield) as the product after purification with silica gel column chromatography (hexane/EtOAc = 50:1 to 5:1) The spectral data were identical with those reported in the literature.[15]

^{1}H NMR (600 MHz, $CDCl_3$) δ 7.35 (m, 2H), 7.33 (m, 2H), 5.08 (m, 1H), 2.60 (m, 1H), 2.43 (m, 1H). **^{19}F NMR** (565 MHz, $CDCl_3$) δ -63.70 (t, *J* = 10.9 Hz). **^{13}C NMR** (151 MHz, $CDCl_3$) δ 140.74, 134.19, 129.02, 128.50, 125.7 (q, *J* = 278 Hz), 68.24, 42.9 (q, *J* = 27.1 Hz).

3,3,3-trifluoro-1-(4-(hydroxymethyl) phenyl) propan-1-ol **(9)**:

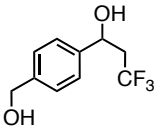

According to the default condition, compound **9** was synthesized according to the same procedure described for compound **3**, yielding a colorless oil (16.5 mg, 75% yield) as the product after purification with silica gel column chromatography (hexane/EtOAc = 50:1 to 0:1)

^{1}H NMR (600 MHz, $CDCl_3$) δ 7.37 (s, 4H), 5.08 (dd, *J* = 9.0, 3.7 Hz, 1H), 4.70 (s, 2H), 2.74 - 2.56 (m, 1H), 2.55 - 2.35 (m, 1H). **^{19}F NMR** (565 MHz, $CDCl_3$) δ -63.69 (t, *J* = 10.7 Hz). **^{13}C NMR** (151 MHz, $CDCl_3$) δ 141.76, 141.09, 127.41, 126.59 (q, *J* = 270 Hz), 125.92, 68.60, 64.91, 42.88 (q, *J* = 26.9 Hz). ESI$^+$-HRMS: $[M+NH_4]^+$ calcd. for $C_{10}H_{15}F_3O_2N$: 238.1049; Found 238.1050.

4-(3,3,3-trifluoro-1-hydroxypropyl) benzonitrile **(10)**:[17]

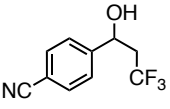

According to default condition, compound **10** was synthesized according to the same procedure described for compound **3**, yielding a colorless oil (12.5 mg, 58% yield) as the product after purification with silica gel column chromatography (hexane/EtOAc = 50:1 to 5:1) The spectral data were identical with those reported in the literature.[17]

^{1}H NMR (600 MHz, $CDCl_3$) δ 7.68 (d, *J* = 8.4 Hz, 2H), 7.56 - 7.48 (m, 2H), 5.16 (dd, *J* = 8.9, 3.6 Hz, 1H), 2.68 - 2.54

(m, 1H), 2.53 - 2.40 (m, 1H). **^{19}F NMR** (565 MHz, $CDCl_3$) δ -63.60 (t, *J* = 10.5 Hz). **^{13}C NMR** (151 MHz, $CDCl_3$) δ 147.28, 132.67, 126.46, 125.39 (q, *J* = 270 Hz), 118.44, 112.23, 68.13, 42.92 (q, *J* = 27.2 Hz).

4-(3,3,3-trifluoro-1-hydroxypropyl) benzoic acid **(11)**:[18]

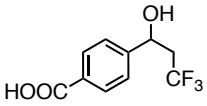

According to default condition, compound **11** was synthesized according to the same procedure described for compound **3**, yielding a white solid (17.3 mg, 74% yield) as the product after purification with silica gel column chromatography (hexane/EtOAc = 50:1 to 0:1) The spectral data were identical with those reported in the literature.[18]

^{1}H NMR (600 MHz, MeOD) δ 8.02 (d, *J* = 8.3 Hz, 2H), 7.51 (d, *J* = 8.2 Hz, 2H), 5.06 (s, 1H), 2.76 - 2.39 (m, 2H). **^{19}F NMR** (565 MHz, MeOD) δ -64.94 (t, *J* = 10.6 Hz). **^{13}C NMR** (151 MHz, MeOD) δ 168.17, 148.60, 130.11, 129.06, 126.98, 126.11, 125.07, 68.00, 67.01, 40.95.

3,3,3-trifluoro-2-methyl-1-phenylpropan-1-ol **(12)**:[15]

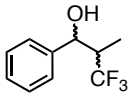

According to default condition, compound **12** was synthesized according to the same procedure described for compound **3**, yielding a colorless oil (12.7 mg, 63% yield) as the product after purification with silica gel column chromatography (hexane/EtOAc = 50:1 to 5:1) The spectral data were identical with those reported in the literature.[15]

^{1}H NMR (600 MHz, $CDCl_3$) δ 7.48 - 7.27 (m, 5H), 5.23 (t, *J* = 3.1 Hz, 1H), 4.82 (dd, *J* = 8.2, 2.8 Hz, 1H), 2.72 - 2.59 (m, 1H), 2.55 - 2.32 (m, 1H), 2.16 (d, *J* = 3.1 Hz, 1H), 1.94 (d, *J* = 3.5 Hz, 1H), 1.09 (d, *J* = 7.1 Hz, 2H), 0.87 (d, *J* = 7.2 Hz, 2H). **^{19}F NMR** (565 MHz, $CDCl_3$) δ -68.60 (d, *J* = 8.0 Hz), -70.13 (d, *J* = 9.0 Hz). **^{13}C NMR** (151 MHz, $CDCl_3$) δ 141.49, 140.94, 128.68, 128.64, 128.68, 127.78, 126.97, 125.64, 74.03, 70.56, 44.5 - 45.6 (m), 29.72, 10.57, 5.88.

Reaction conditions for the hydroxytrifluoromethylation of compound 14:

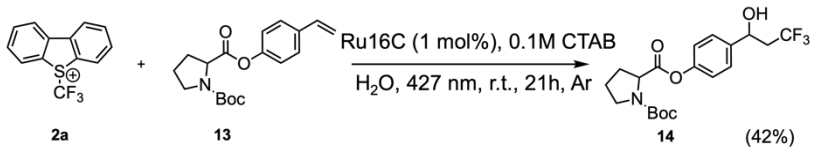

The photocatalytic reaction was carried in a reaction tube equipped with a magnetic stir bar at room temperature. Ru16C (0.85 mg, 0.01 mmol), 5-(trifluoromethyl) dibenzothiophenium tetrafluoroborate (Umemoto's reagent, **2a**) (34 mg, 0.1 mmol), **4** (34.9 mg, 0.11 mmol) and 0.1 M CTAB in water (2 ml) were added into the reaction tube. The obtained solution was purged with Argon for three minutes and dipped into a water bath to maintain a stable temperature. An extra fan was equipped on the top of the reaction tube, and a 427 nm LED was placed about 3 cm away from it. The yellow solution was stirred at room temperature under a 427 nm LED irradiation. After 21 hours, the reaction mixture was extracted with methyl *tert*-butyl ether twice. The combined organic solution was dried by adding Na_2SO_4 and filtrated. The filtrate was concentrated under vacuum, and the organic solvent was removed through rotary evaporation. The resulting liquid was purified by silica gel chromatography using hexane: EtOAc= (5:0 to 5:1) as the eluent, yielding a yellow oil product that was dried in a vacuum oven at 40 °C. (16.9 mg, 42% yield)

1-(*tert*-butyl) 2-(4-(3,3,3-trifluoro-1-hydroxypropyl)phenyl) pyrrolidine-1,2-dicarboxylate (**14**):

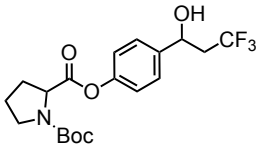

^{1}H NMR (600 MHz, $CDCl_3$) δ 7.39 (d, *J* = 8.4 Hz, 1H), 7.34 (d, *J* = 8.3 Hz, 1H), 7.11 - 6.99 (m, 2H), 5.12 - 4.95 (m, 1H), 4.45 (m, 1H), 3.63 - 3.34 (m, 2H), 2.86 (s, 1H), 2.65 - 2.50 (m, 1H), 2.50 - 2.21 (m, 2H), 2.14 (m, 1H), 2.09 - 1.78 (m, 2H), 1.51 - 1.26 (m, 9H). **^{13}C NMR** (151 MHz, $CDCl_3$) δ 171.65, 171.61, 154.56, 153.82, 150.52, 150.32, 140.37, 140.23, 126.94, 126.78, 124.74 (q, *J* = 280 Hz), 121.80, 121.46, 80.41, 80.18, 68.15, 68.12, 68.10, 68.07, 59.20, 59.06, 46.67, 46.45, 43.06, 43.01, 42.84, 42.79, 42.62, 31.03, 30.01, 28.40, 24.49, 23.70. ESI^+-HRMS: $[M+H]^+$ calcd. for $C_{14}H_{16}F_3NO_3$: 304.1082; Found 304.1160.

Reaction set up:

Figure S7. Reaction apparatus of hydroxytrifluoromethylation irradiated under 427 nm. (LED light source: Kessil LEDs 427 nm)

9. Substrates with low conversion or that remain unreactive under default conditions

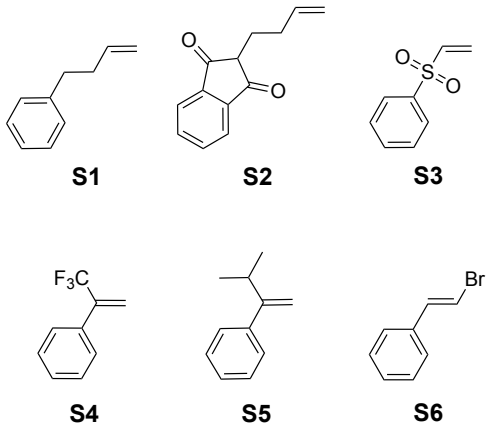

Substrates such as phenyl vinyl sulfone and poly-substituted olefins (S3, S5) exhibited low conversion rates (10-30%) under standard reaction conditions, while unactivated terminal olefins substrates (S1, S2) and other substrates (S4, S6) yielded only trace products with most starting material remaining.

10. TEMPO-trapping experiment study

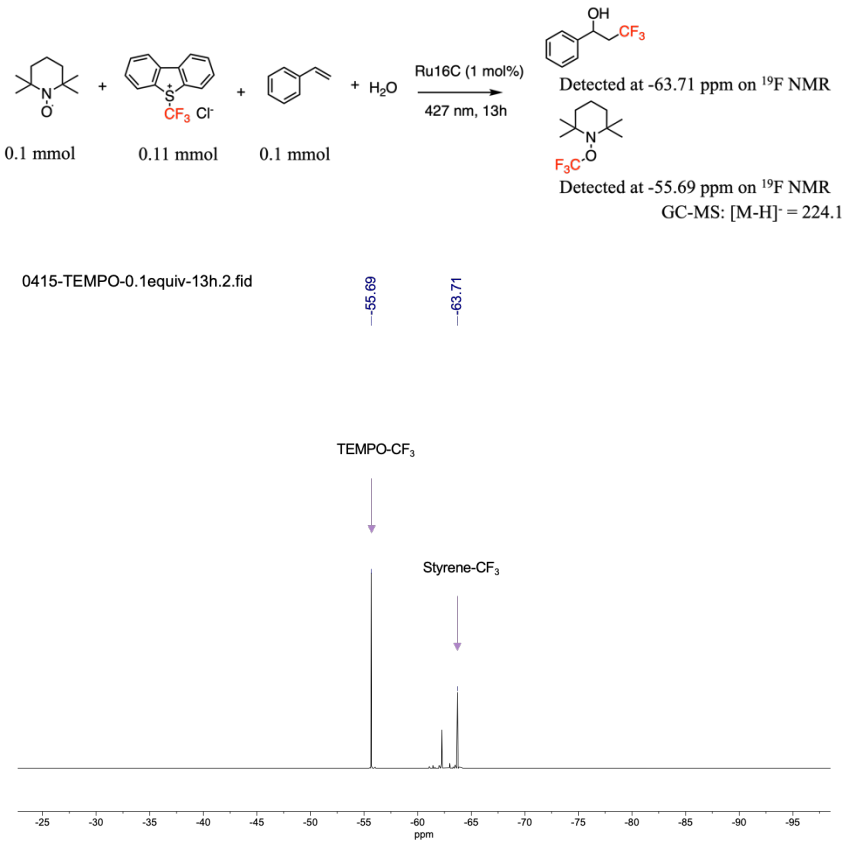

Figure S8. ^{19}F NMR of TEMPO-adduct after photocatalysis for 13 hours in $CDCl_3$.

11. Reaction condition of hydroxylation of aryl boronic acids

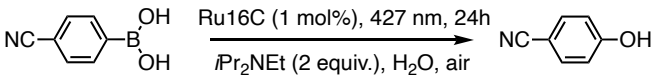

15 **16** (78%)

The photocatalytic reaction was carried in a reaction tube equipped with a magnetic stir bar. Ru16C (0.85 mg, 0.01 mmol), 4-cyanophenyl)boronic acid (**15**) (14.7 mg, 0.1 mmol), *N*,*N*-Diisopropylethylamine (25.8 mg, 0.2 mmol) and water (1 ml) were added into the reaction tube. An extra fan was equipped on the top of the reaction tube, and a 427 nm LED was placed about 3 cm away from it. The yellow solution was stirred at room temperature under a 427 nm LED irradiation. After 24 hours, the reaction mixture was extracted with methyl *tert*-butyl ether three times. The combined organic solution was dried by adding Na_2SO_4 and filtrated. The filtrate was concentrated under vacuum. The isolated product was obtained by silica gel chromatography using hexane: EtOAc= (10:0 to 3:1) as the eluent, yielding a white powder product that was dried in a vacuum oven at 40 °C. (9.3 mg, 78% yield) 4-hydroxybenzonitrile (**16**): The spectral data were identical to those reported in the literature.[19]

^1H NMR (600 MHz, $CDCl_3$) δ 7.56 (d, J = 8.9 Hz, 2H), 7.54 (d, J = 8.9 Hz, 2H), 6.49 (s, 1H). ^{13}C NMR (151 MHz, $CDCl_3$) δ 160.06, 134.56, 134.34, 134.09, 119.23, 116.45, 103.29.

12. Catalyst Recycling

Catalyst recovery procedure: given the stability of ruthenium complexes, the Ru16C catalyst was efficiently recovered using an additional mini pipette column packed with 300 mg of Al_2O_3 after the completion of the reaction and before the purification of product **3** (Figure S9). A solvent mixture of hexane:EtOAc (1:1, 8 mL) was applied, followed by acetonitrile:water (10:1, 1 mL), enabling the successful purification of the catalyst. This process achieved an 80% recovery of the Ru16C used in the reaction. After applying the hexane:EtOAc (1:1, 8 mL) and acetonitrile:water (10:1, 1 mL) mixtures to recover the Ru16C catalyst, the hexane and ethyl acetate mixture was collected and concentrated under vacuum. Product **3** was then purified from this concentrated mixture using a separate column purification step, achieving an 84% isolation yield. The recycled catalyst was subsequently tested under standard reaction conditions, yielding product **3** with an 82% isolation yield, which confirms Ru16C retains its activity after recovery.

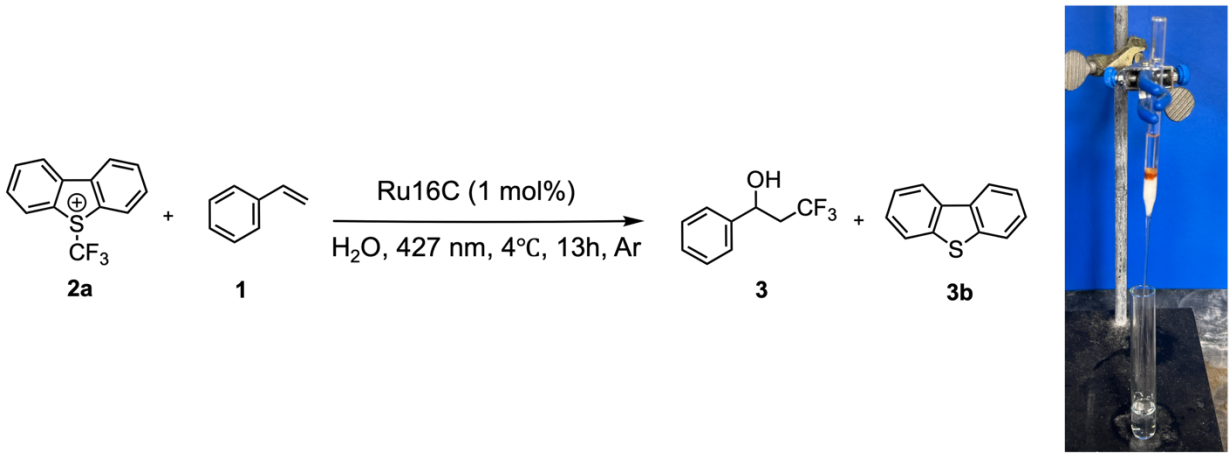

Figure S9. Catalyst recovery

13. E-factor Determination

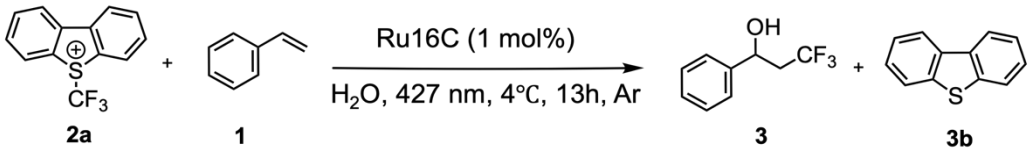

Ru16C (0.85 mg, 0.01 mmol), Umemoto's reagent, **2c** (28.9 mg, 0.1 mmol), styrene (**1**) (11.5 mg, 0.11 mmol), and water (2 ml) were added into the reaction tube. The obtained solution was purged with Argon for three minutes and dipped into a water bath to maintain a stable temperature. The resulting mixture was irradiated by a 427 nm LED at a 4 °C fridge. After 13 hours, the reaction mixture was extracted with methyl *tert*-butyl ether twice (0.2 ml). The combined organic solution was dried by adding Na_2SO_4 and filtrated. The isolated product was obtained by silica gel chromatography, yielding a colorless oil product. (15.6 mg, 82% yield).

E factor calculation $= \frac{total\ waste\ (kg)}{total\ product\ (kg)}$

$= \frac{MTBE\ (extraction) + by\ product\ (3b)}{isolated\ product\ (3)}$

$= \frac{147.2\ mg + 18.4\ mg}{15.2\ mg}$

= 10.9

Similar reactions conducted in organic solvents using $Ru(bpy)_3(PF_6)_2$ were evaluated based on previously reported literature and procedures in reference[15]

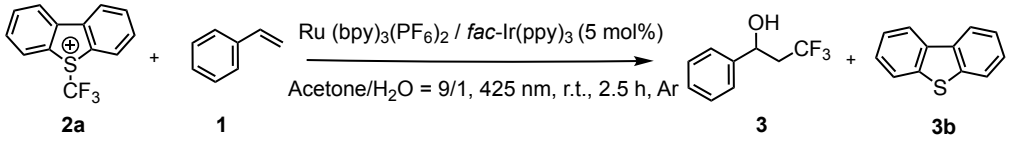

(calculated based on using 0.1 mmol styrene)

E factor calculation = $\frac{total\ waste\ (kg)}{total\ product\ (kg)}$

$= \frac{DCM\ (extraction) + by\ product\ (3b) + acetone\ (reaction)}{isolated\ product\ (3)}$

$= \frac{266\ mg + 18.4\ mg + 706.1\ mg}{16.8\ mg}$

= 37.9

Note: The volume of DCM used for product extraction was assumed to be the same as in our procedure, as this information was not reported in the literature[15]

Moreover, the E factor for the same transformation, using an alternative synthetic strategy, was calculated based on the reported literature and procedures[16]

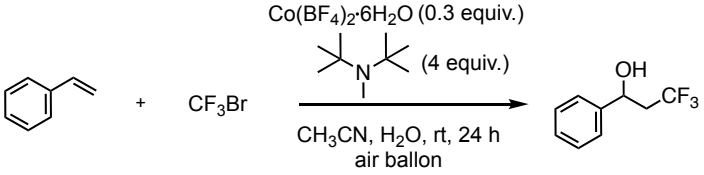

(calculated based on using 0.1 mmol styrene)

E factor calculation = $\frac{total\ organic\ waste\ (kg)}{total\ product\ (kg)}$

$= \frac{DCM\ and\ Et_2O\ (extraction) + acetonritle\ (reaction) + amine + Co\ salt + by\ product\ (HBr)}{isolated\ product\ (3)}$

$= \frac{1.995\ g + 1.065g + 0.313g + 51.7\ mg + 10.3\ mg + 6.8\ mg}{16.0\ mg}$

= 215.1

Note: As volumes of solvents for chromatography are typically not reported in the literature and will also depend on the operator's skills, these are not used in the E factor calculation here. This is consistent with Bu et al. (M. Bu, C. Cai, F. Gallou and B. H. Lipshutz, *Green Chem.*, **2018**, 20, 1233–1237, Ref. 34 in the main manuscript).

14. References

1 K. Suzuki, A. Kobayashi, S. Kaneko, K. Takehira, T. Yoshihara, H. Ishida, Y. Shiina, S. Oishi and S. Tobita, *Phys. Chem. Chem. Phys.*, 2009, **11**, 9850.
2 R. Danev and W. Baumeister, *Curr. Opin. Struct. Biol.*, 2017, **46**, 87–94.
3 S. P. Morcillo, L. Álvarez de Cienfuegos, A. J. Mota, J. Justicia and R. Robles, *J. Org. Chem.*, 2011, **76**, 2277–2281.
4 B. P. Sullivan, D. J. Salmon and T. J. Meyer, *Inorg. Chem.*, 1978, **17**, 3334–3341.
5 J. R. Bellare, H. T. Davis, L. E. Scriven and Y. Talmon, *J. Electron Microsc. Tech.*, 1988, **10**, 87–111.
6 H. Sternlicht, G. C. Nieman and G. W. Robinson, *J. Chem. Phys.*, 1963, **38**, 1326–1335.
7 R. Knoesel, D. Markovitsi, J. Simon and G. Duportail, *J. Photochem.*, 1983, **22**, 275–283.
8 P. Kubát and J. Mosinger, *J. Photochem. Photobiol. Chem.*, 1996, **96**, 93–97.
9 S. Kajouj, L. Marcélis, V. Lemaur, D. Beljonne and C. Moucheron, *Dalton Trans.*, 2017, **46**, 6623–6633.
10 S. Estalayo-Adrián, S. Blasco, S. A. Bright, G. J. McManus, G. Orellana, D. C. Williams, J. M. Kelly and T. Gunnlaugsson, *ACS Appl. Bio Mater.*, 2021, acsabm.1c00284.
11 K. Suzuki, A. Kobayashi, S. Kaneko, K. Takehira, T. Yoshihara, H. Ishida, Y. Shiina, S. Oishi and S. Tobita, *Phys. Chem. Chem. Phys.*, 2009, **11**, 9850.
12 M. Kubista, R. Sjöback, S. Eriksson and B. Albinsson, *The Analyst*, 1994, **119**, 417–419.
13 G. A. Crosby and J. N. Demas, *J. Phys. Chem.*, 1971, **75**, 991–1024.
14 A. M. Brouwer, *Pure Appl. Chem.*, 2011, **83**, 2213–2228.
15 Y. Yasu, T. Koike and M. Akita, *Angew. Chem. Int. Ed.*, 2012, **51**, 9567–9571.
16 Q. Li, W. Fan, D. Peng, B. Meng, S. Wang, R. Huang, S. Liu and S. Li, *ACS Catal.*, 2020, **10**, 4012–4018.
17 W. Jud, C. O. Kappe and D. Cantillo, *Chem. – Eur. J.*, 2018, **24**, 17234–17238.
18 B. K. Kundu, C. Han, P. Srivastava, S. Nagar, K. E. White, J. A. Krause, C. G. Elles and Y. Sun, *ACS Catal.*, 2023, **13**, 8119–8127.
19 Y. Q. Zou, J. R. Chen, X. P. Liu, L. Q. Lu, R. L. Davis, K. A. Jørgensen and W. J. Xiao, *Angew. Chem. - Int. Ed.*, 2012, **51**, 784–788.

NMR data for all compounds

Bis(bipyridine)ruthenium (hexyl 4'-methyl-[2,2'-bipyridine]-4-carboxylate) (**Ru6C**)

^{1}H NMR of

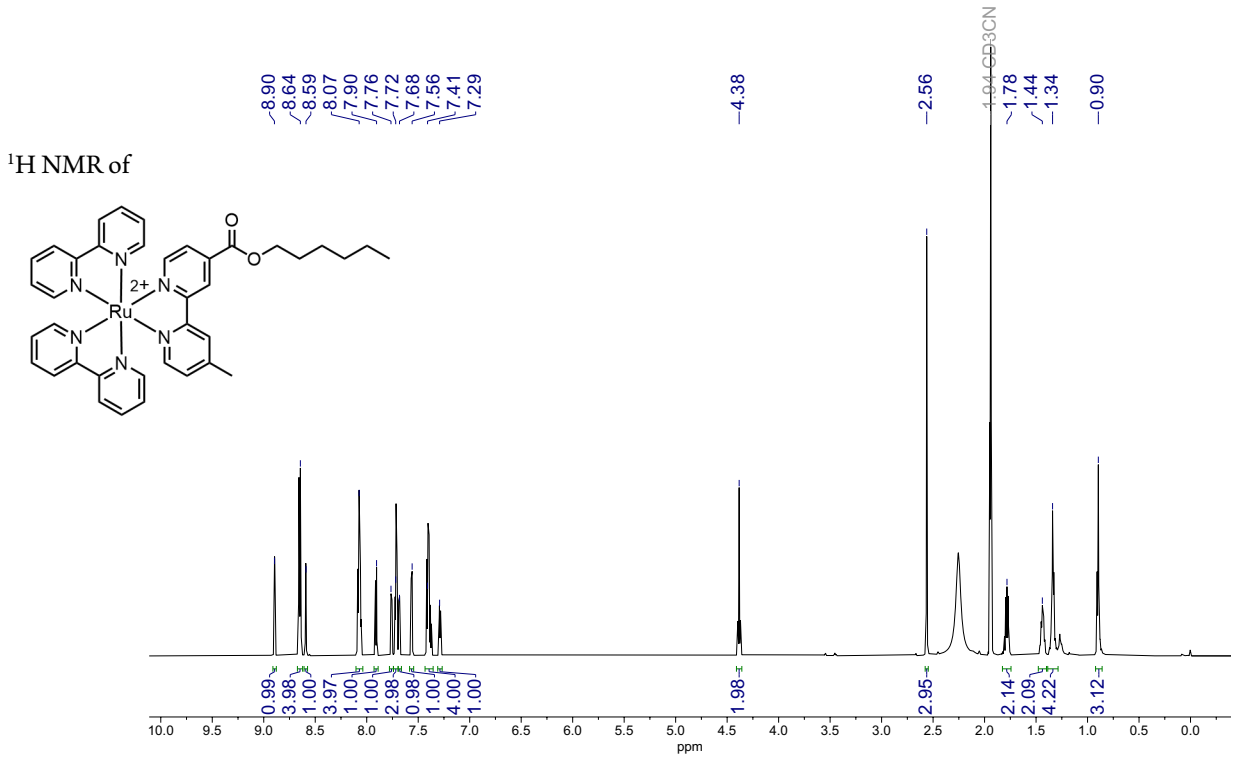

^{13}C NMR of

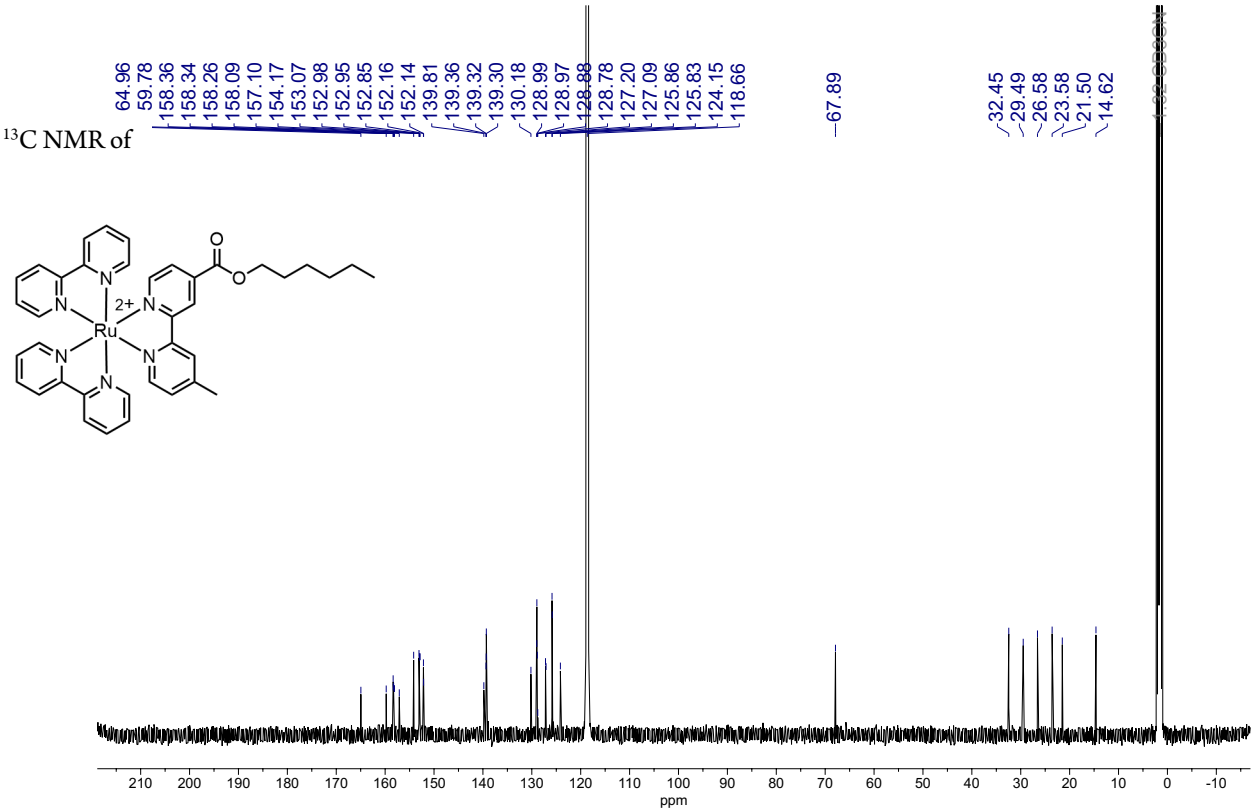

Bis(bipyridine)ruthenium (decyl 4'-methyl-[2,2'-bipyridine]-4-carboxylate) (**Ru10C**)

^{1}H NMR of

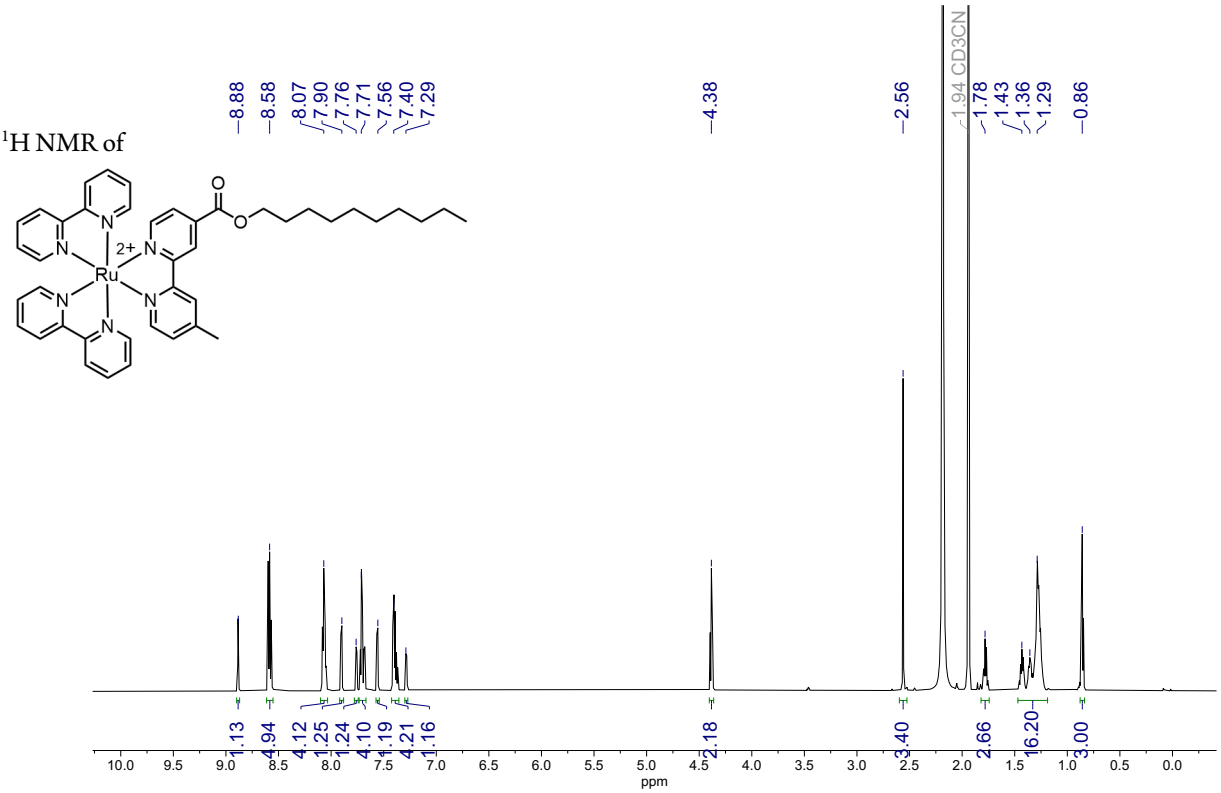

^{13}C NMR of

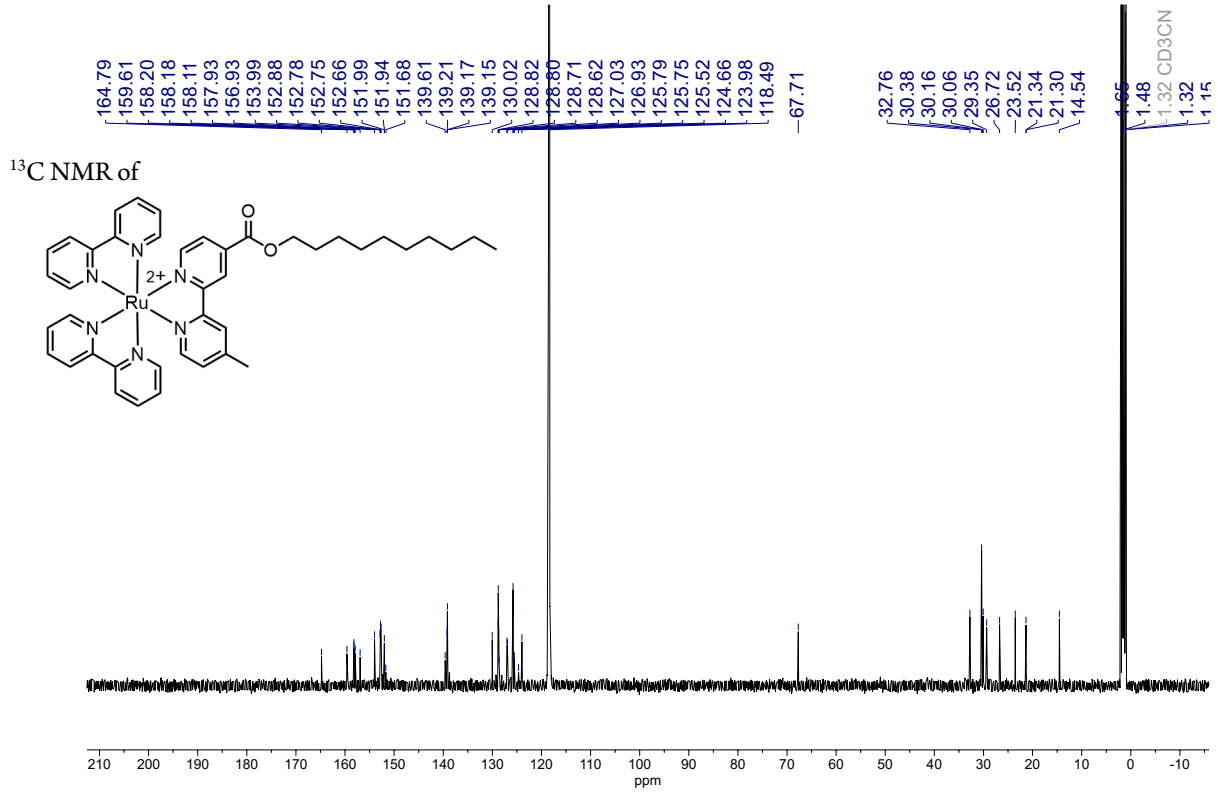

Bis(bipyridine)ruthenium (dodecyl 4'-methyl-[2,2'-bipyridine]-4-carboxylate) (**Ru12C**)

^{1}H NMR of

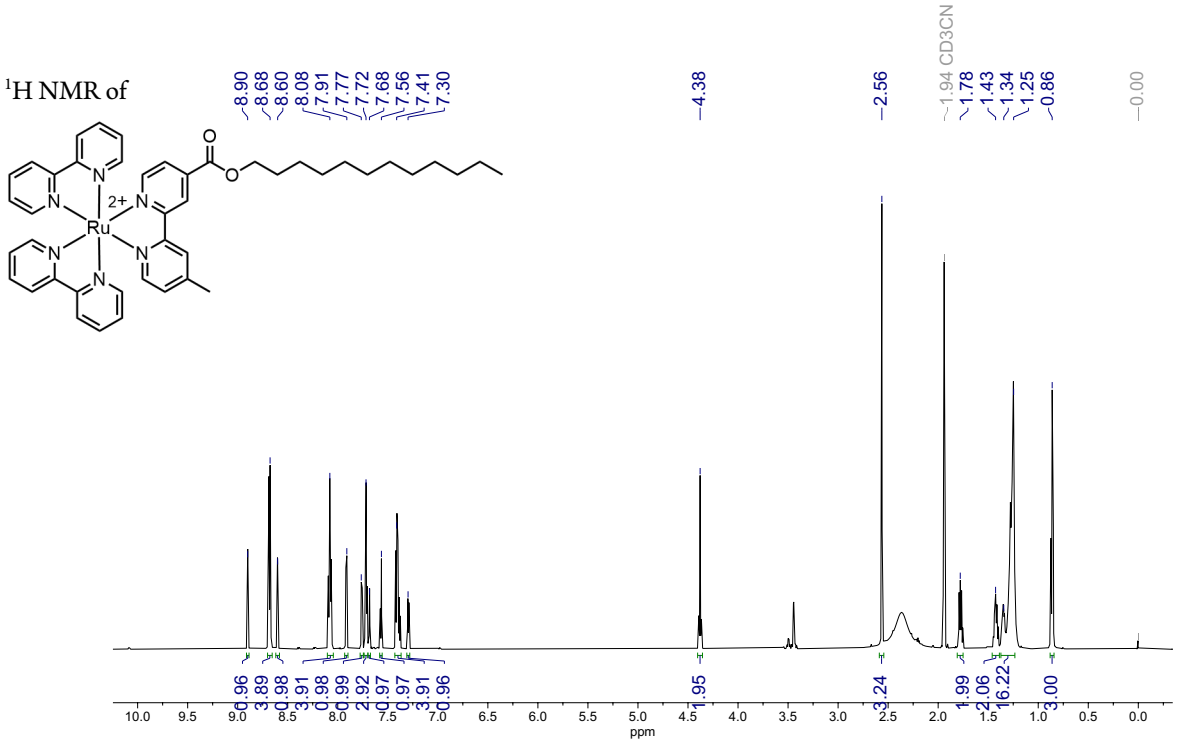

^{13}C NMR of

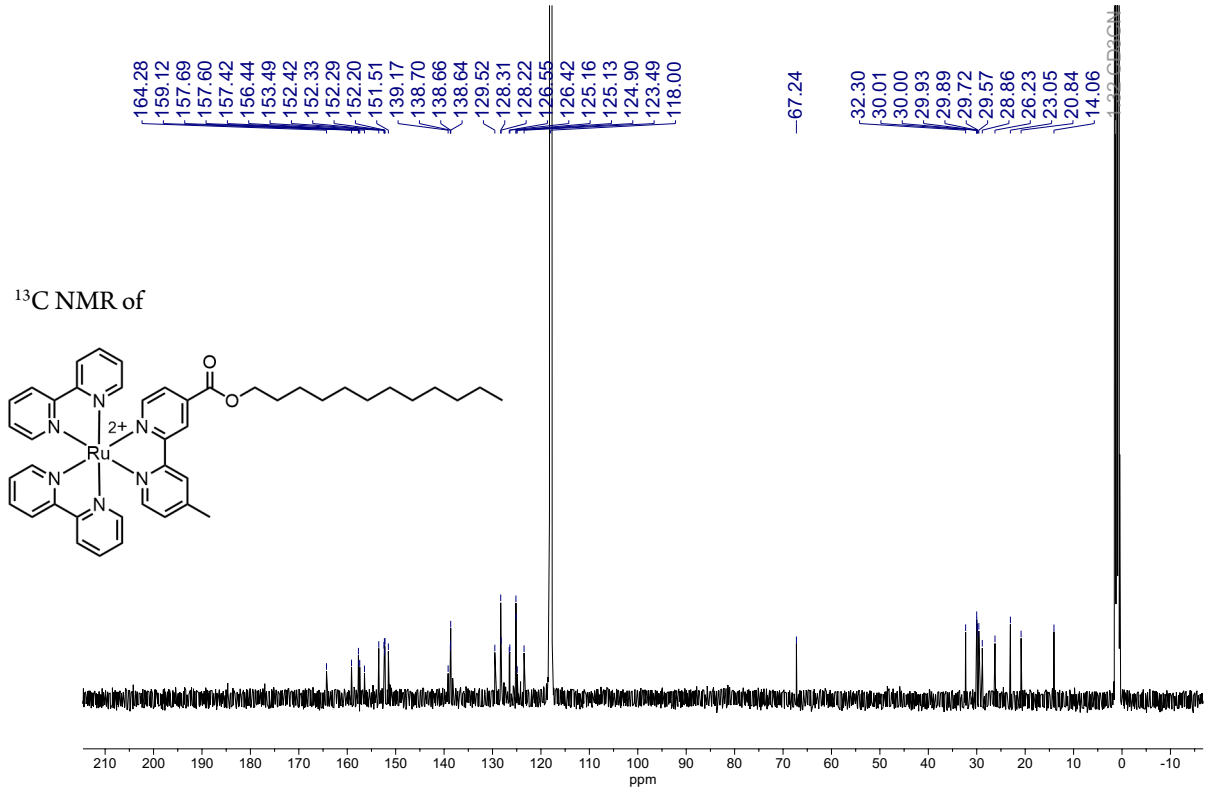

Bis(bipyridine)ruthenium (hexadecyl 4'-methyl-[2,2'-bipyridine]-4-carboxylate) (**Ru16C**)

^{1}H NMR of

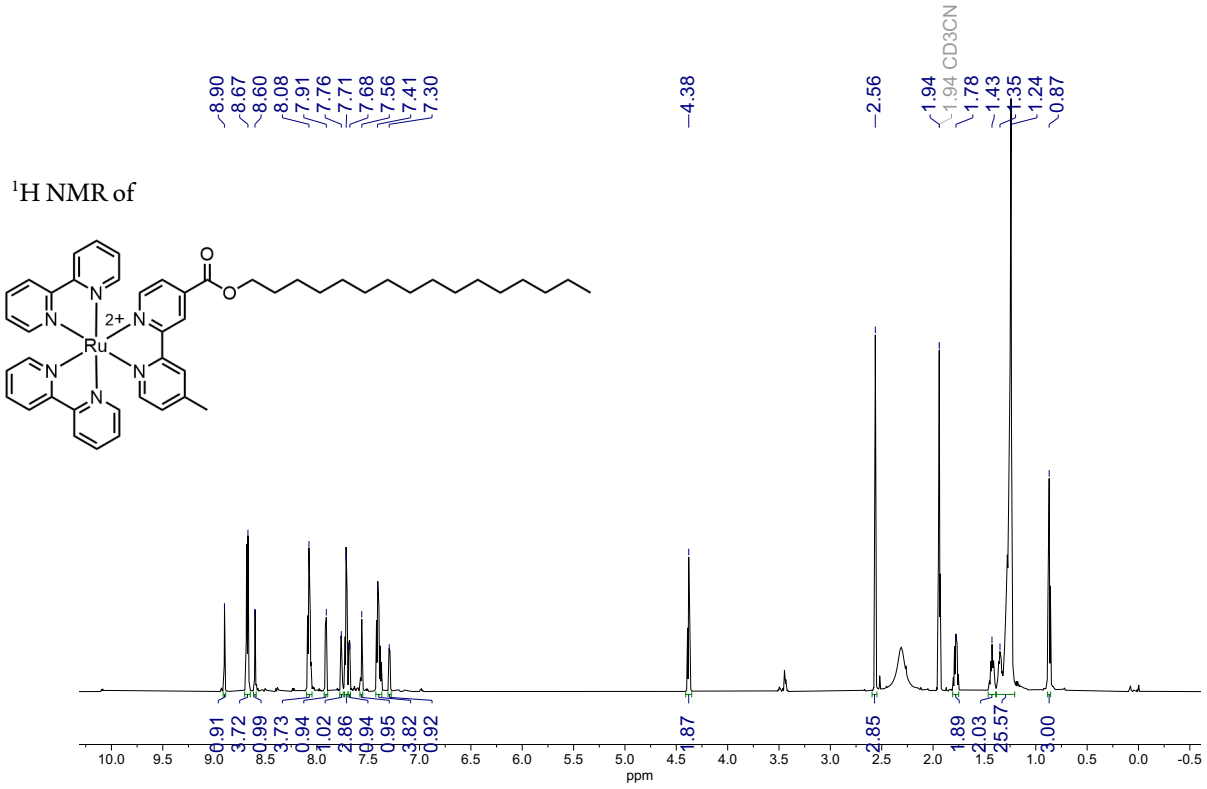

^{13}C NMR of

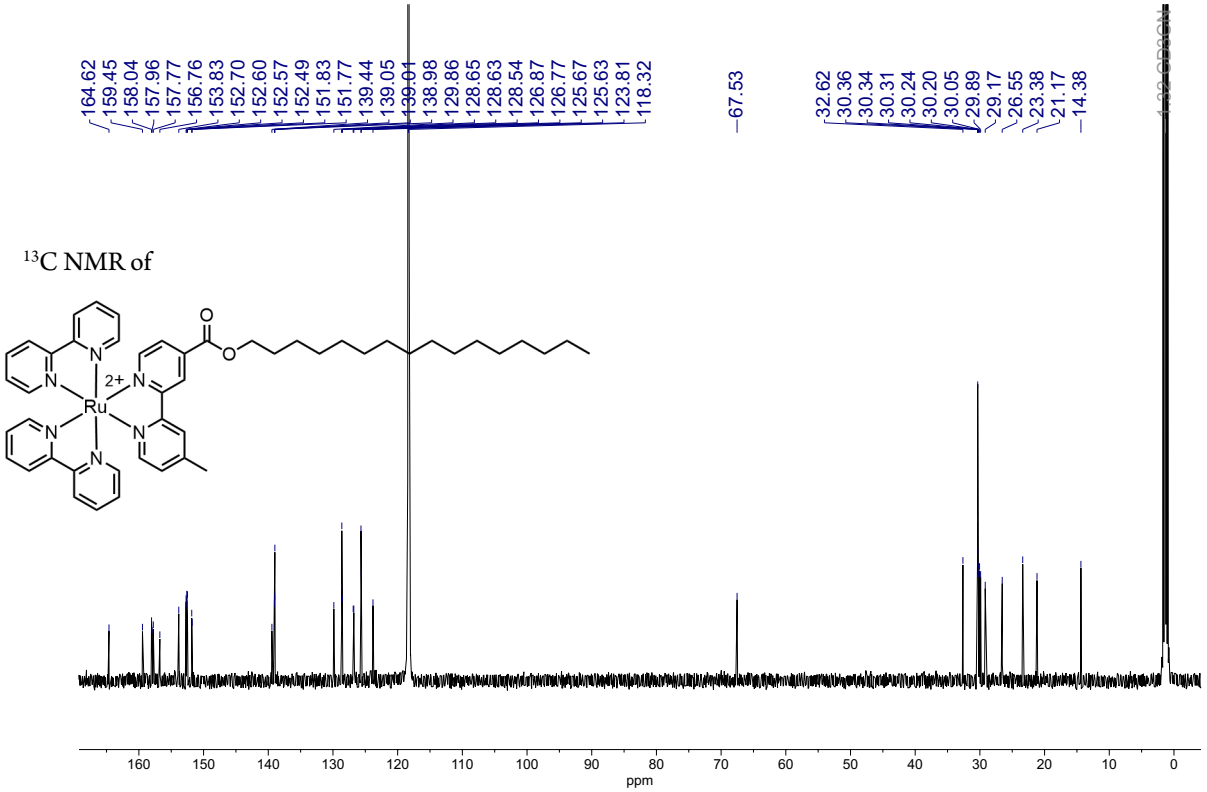

3,3,3-trifluoro-1-phenylpropan-1-ol **(3)**

^{1}H NMR of

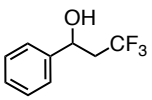

^{19}F NMR of

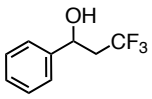

^{13}C NMR of

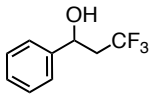

3,3,3-trifluoro-1-(p-tolyl)propan-1-ol **(4)**

^{1}H NMR of

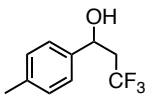

^{19}F NMR of

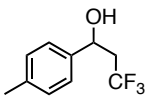

^{13}C NMR of

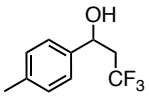

1-(4-(*tert*-butyl)phenyl)-3,3,3-trifluoropropan-1-ol **(5)**

^{1}H NMR of

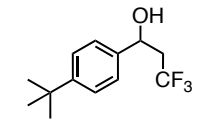

^{19}F NMR of

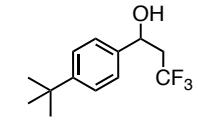

^{13}C NMR of

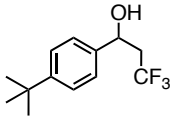

3,3,3-trifluoro-1-(4-methoxyphenyl)propan-1-ol **(6)**

^{1}H NMR of

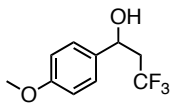

^{19}F NMR of

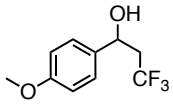

^{13}C NMR of

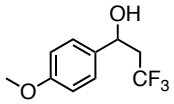

3,3,3-trifluoro-1-(4-fluorophenyl)propan-1-ol **(7)**

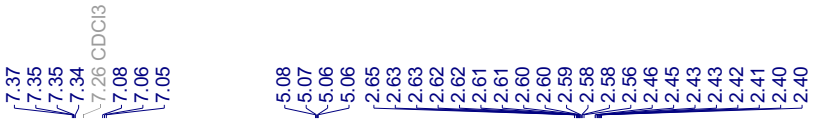

^{1}H NMR of

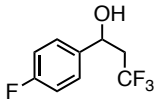

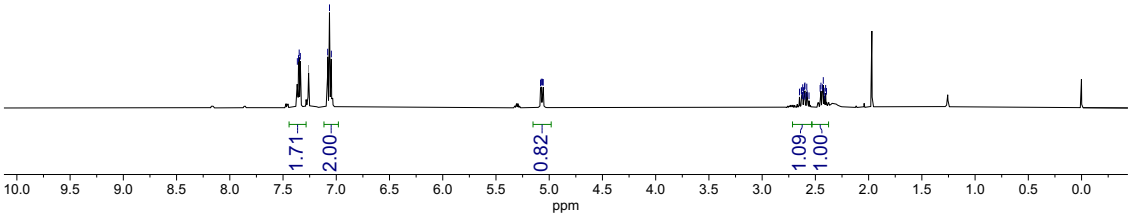

^{19}F NMR of

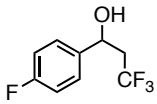

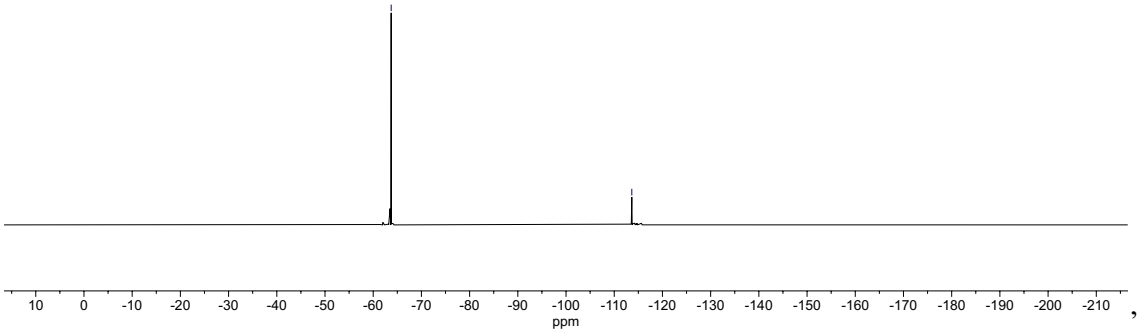

,

^{13}C NMR of

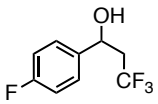

1-(4-chlorophenyl)-3,3,3-trifluoropropan-1-ol **(8)**

^{1}H NMR of

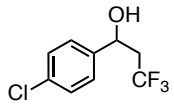

^{19}F NMR of

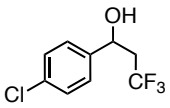

^{13}C NMR of

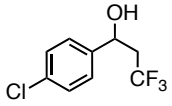

3,3,3-trifluoro-1-(4-(hydroxymethyl)phenyl)propan-1-ol **(9)**

^{1}H NMR of

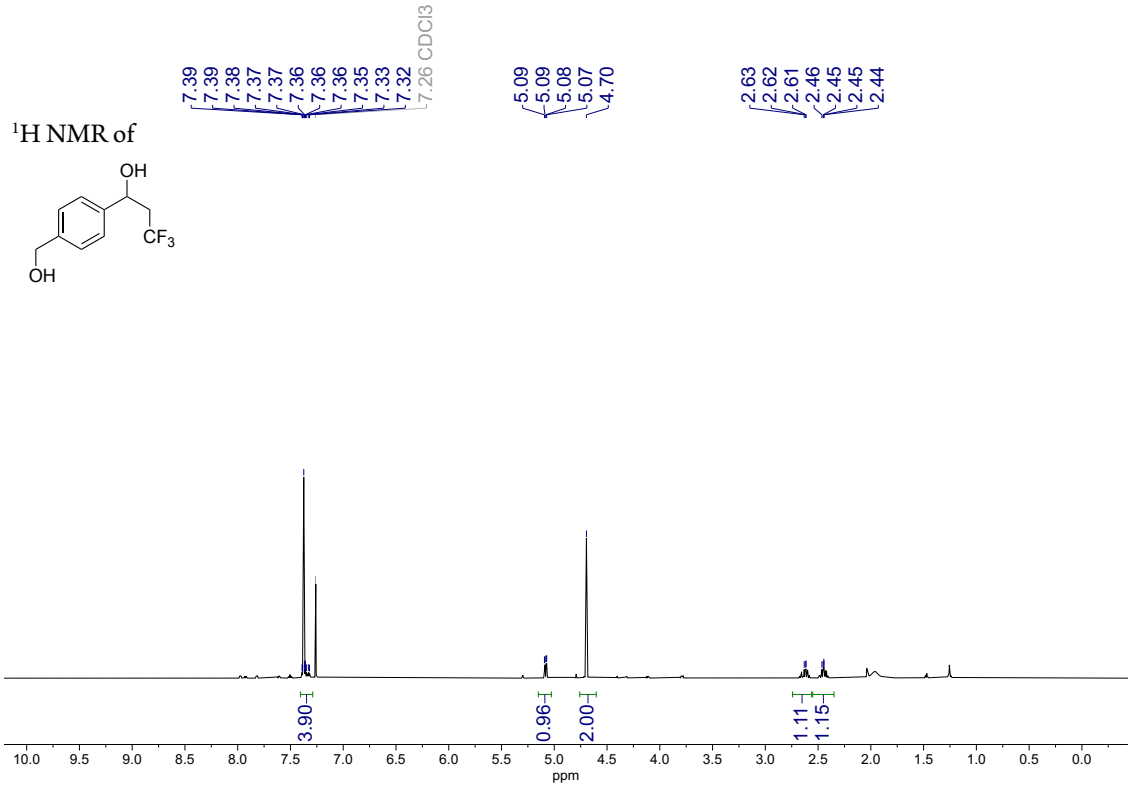

^{19}F NMR of

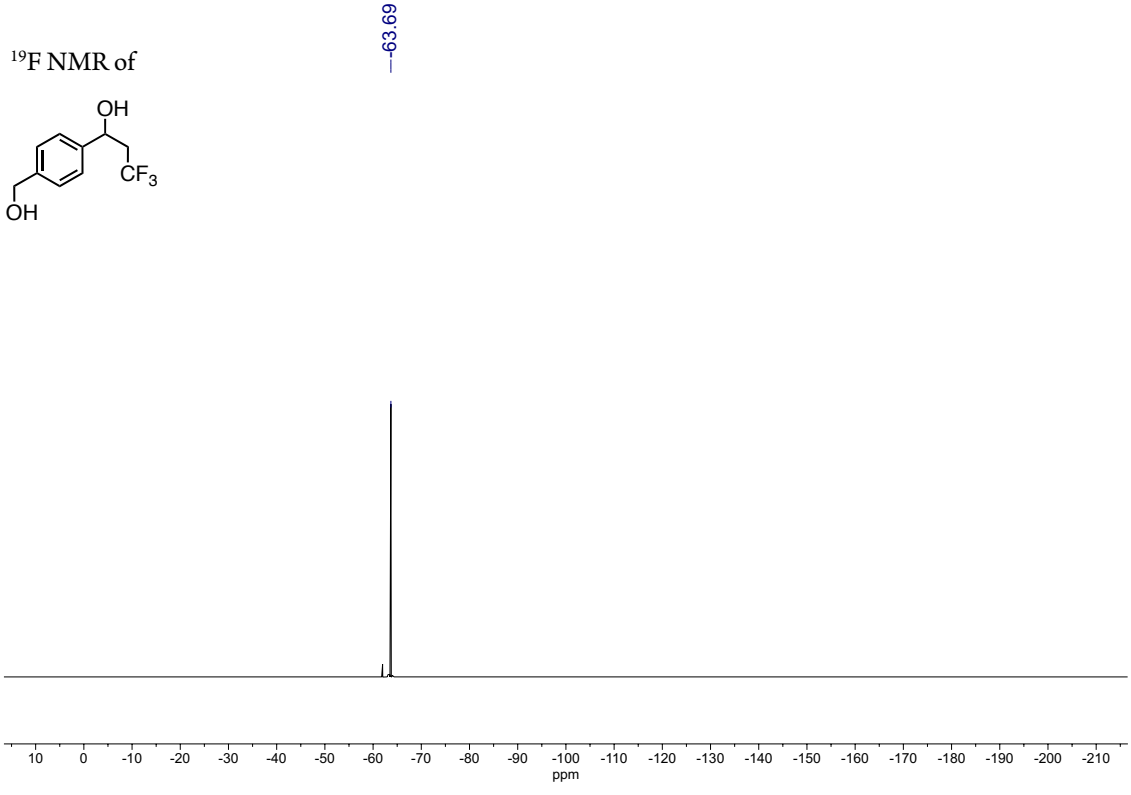

^{13}C NMR of

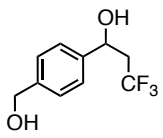

4-(3,3,3-trifluoro-1-hydroxypropyl)benzonitrile **(10)**

^{1}H NMR of

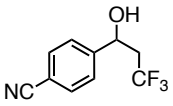

^{19}F NMR of

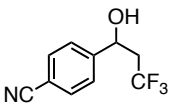

^{13}C NMR of

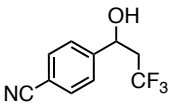

4-(3,3,3-trifluoro-1-hydroxypropyl)benzoic acid **(11)**

^{1}H NMR of

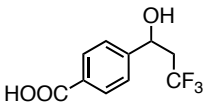

^{19}F NMR of

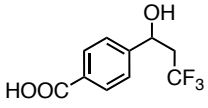

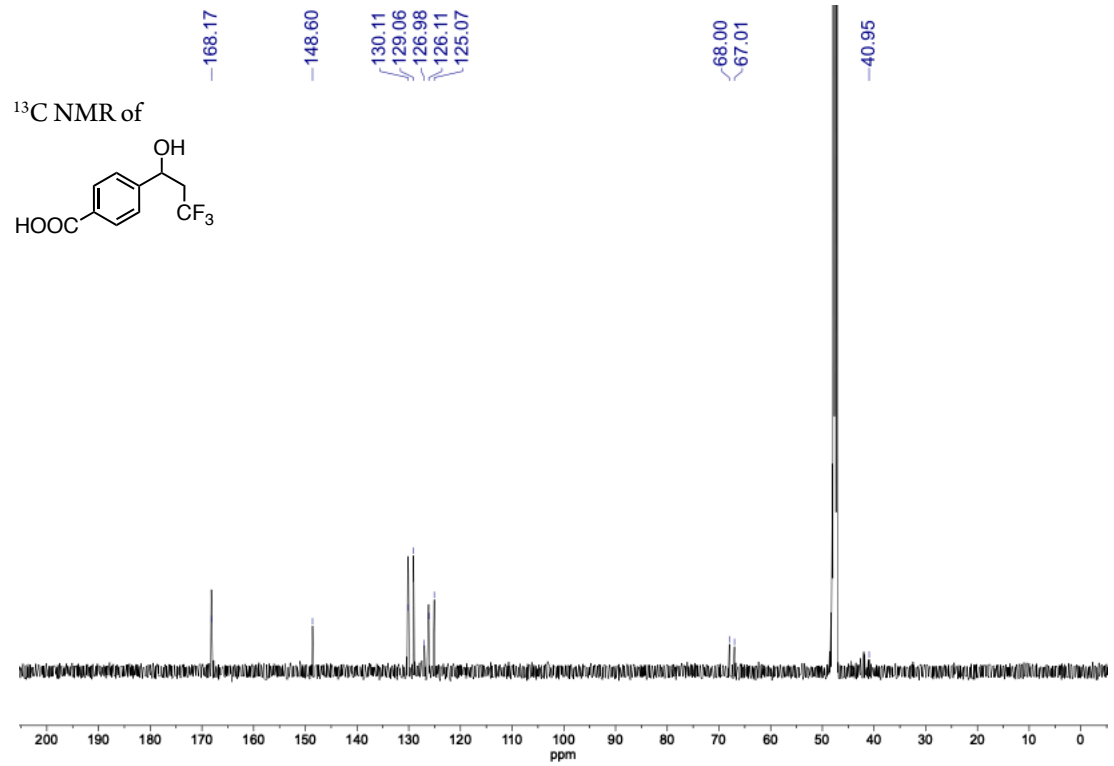

(1R,2S)-3,3,3-trifluoro-2-methyl-1-phenylpropan-1-ol **(12)**

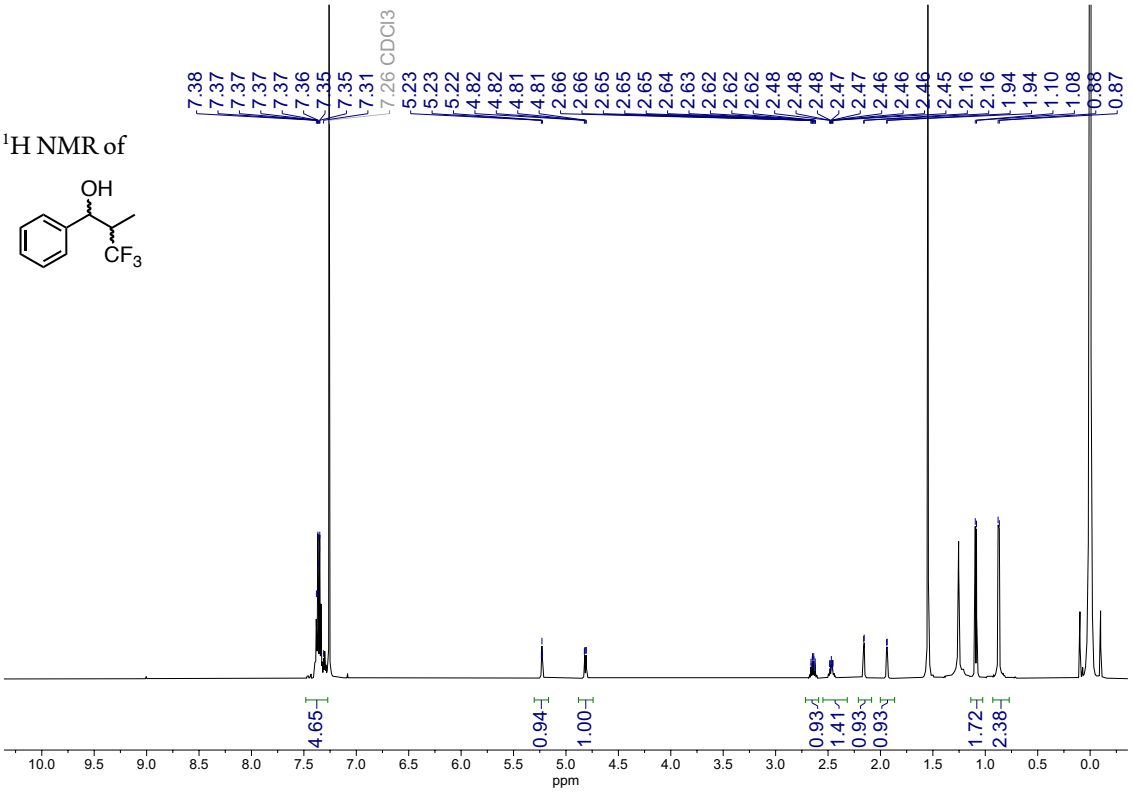

^{19}F NMR of

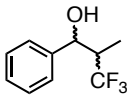

^{13}C NMR of

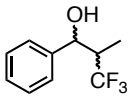

1-(*tert*-butyl) 2-(4-vinylphenyl) pyrrolidine-1,2-dicarboxylate **(13)**

^{1}H NMR of

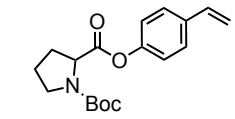

^{13}C NMR of

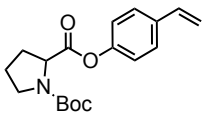

1-(*tert*-butyl) 2-(4-(3,3,3-trifluoro-1-hydroxypropyl)phenyl) pyrrolidine-1,2-dicarboxylate (**14**)

^{1}H NMR of

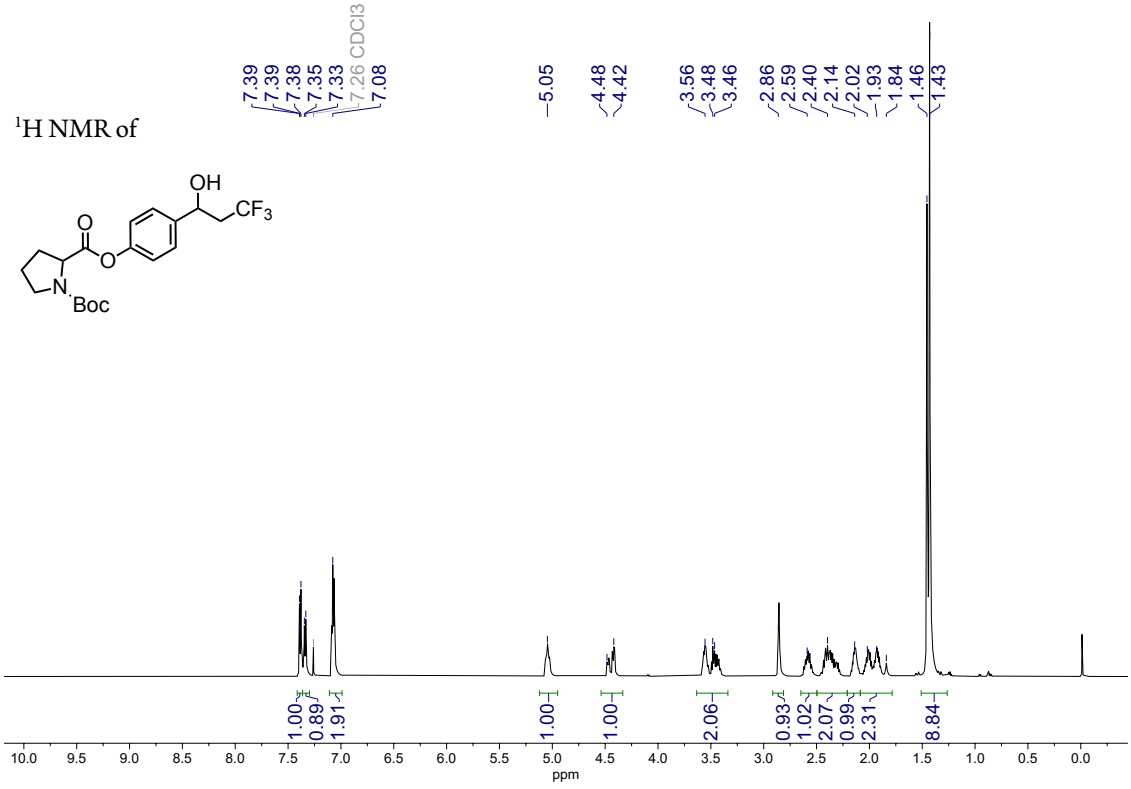

^{19}F NMR of

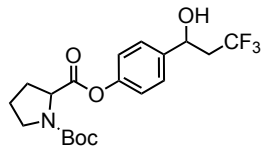

^{13}C NMR of

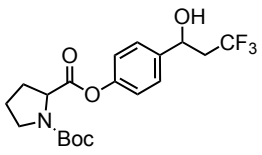

^{1}H NMR of

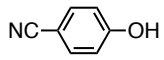

^{13}C NMR of